Inorganic Chemistry

Article

pubs.acs.org/IC

Differential Coordination Demands in Fe versus Mn Water-Soluble Cationic Metalloporphyrins Translate into Remarkably Different Aqueous Redox Chemistry and Biology

Artak Tovmasyan,[†] Tin Weitner,[†] Huaxin Sheng,[‡,∥] MiaoMiao Lu,[‡,∥,§] Zrinka Rajic,[†] David S. Warner,[‡,∥] Ivan Spasojevic,[⊥] Julio S. Reboucas,[#] Ludmil Benov,*[,○] and Ines Batinic-Haberle*[,†]

[†]Departments of Radiation Oncology, [‡]Anesthesiology, [⊥]Medicine, and [∥]Multidisciplinary Neuroprotection Laboratories, Duke University Medical Center, Durham, North Carolina 27710, United States

[§]Department of Anesthesiology, Second Affiliated Hospital, Zhengzhou University, Henan, China

[#]Departamento de Química, CCEN, Universidade Federal da Paraíba, João Pessoa, PB 58051-900, Brazil

[○]Department of Biochemistry, Kuwait University, Faculty of Medicine, 13110 Safat, Kuwait

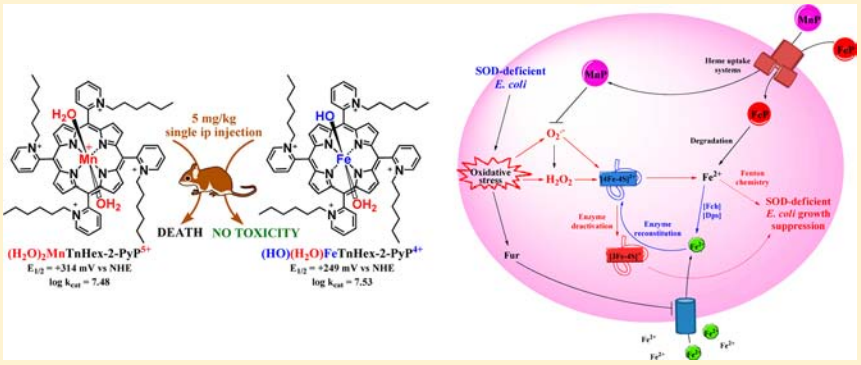

ABSTRACT: The different biological behavior of cationic Fe and Mn pyridylporphyrins in *Escherichia coli* and mouse studies prompted us to revisit and compare their chemistry. For that purpose, the series of *ortho* and *meta* isomers of Fe(III) *meso*-tetrakis-*N*-alkylpyridylporphyrins, alkyl being methyl to *n*-octyl, were synthesized and characterized by elemental analysis, UV/vis spectroscopy, mass spectrometry, lipophilicity, protonation equilibria of axial waters, metal-centered reduction potential, $E_{1/2}$ for $M^{III}P/M^{II}P$ redox couple (M = Fe, Mn, P = porphyrin), k_{cat} for the catalysis of $O_2^{\bullet-}$ dismutation, stability toward peroxide-driven porphyrin oxidative degradation (produced in the catalysis of ascorbate oxidation by MP), ability to affect growth of SOD-deficient *E. coli*, and toxicity to mice. Electron-deficiency of the metal site is modulated by the porphyrin ligand, which renders Fe(III) porphyrins ≥5 orders of magnitude more acidic than the analogous Mn(III) porphyrins, as revealed by the pK_{a1} of axially coordinated waters. The 5 log units difference in the acidity between the Mn and Fe sites in porphyrin translates into the predominance of tetracationic $(OH)(H_2O)$FeP complexes relative to pentacationic $(H_2O)_2$MnP species at pH ~7.8. This is additionally evidenced in large differences in the $E_{1/2}$ values of $M^{III}P/M^{II}P$ redox couples. The presence of hydroxo ligand labilizes trans-axial water which results in higher reactivity of Fe relative to Mn center. The differences in the catalysis of $O_2^{\bullet-}$ dismutation (log k_{cat}) between Fe and Mn porphyrins is modest, 2.5−5-fold, due to predominantly outer-sphere, with partial inner-sphere character of two reaction steps. However, the rate constant for the inner-sphere H_2O_2-based porphyrin oxidative degradation is 18-fold larger for $(OH)(H_2O)$FeP than for $(H_2O)_2$MnP. The *in vivo* consequences of the differences between the Fe and Mn porphyrins were best demonstrated in SOD-deficient *E. coli* growth. On the basis of fairly similar log $k_{cat}(O_2^{\bullet-})$ values, a very similar effect on the growth of SOD-deficient *E. coli* was anticipated by both metalloporphyrins. Yet, while $(H_2O)_2$MnTE-2-PyP^{5+} was fully efficacious at ≥20 μM, the Fe analogue $(OH)(H_2O)$FeTE-2-PyP^{4+} supported SOD-deficient *E. coli* growth at as much as 200-fold lower doses in the range of 0.1−1 μM. Moreover the pattern of SOD-deficient *E. coli* growth was different with Mn and Fe porphyrins. Such results suggested a different mode of action of these metalloporphyrins. Further exploration demonstrated that (1) 0.1 μM $(OH)(H_2O)$FeTE-2-PyP^{4+} provided similar growth stimulation as the 0.1 μM Fe salt, while the 20 μM Mn salt provides no protection to *E. coli*; and (2) 1 μM Fe porphyrin is fully degraded by 12 h in *E. coli* cytosol and growth medium, while Mn porphyrin is not. Stimulation of the aerobic growth of SOD-deficient *E. coli* by the Fe porphyrin is therefore due to iron acquisition. Our data suggest that *in vivo*, redox-driven degradation of Fe porphyrins resulting in Fe release plays a major role in their biological action. Possibly, iron reconstitutes enzymes bearing [4Fe-4S] clusters as active sites. Under the same experimental conditions, $(OH)(H_2O)$FePs do not cause mouse arterial hypotension, whereas $(H_2O)_2$MnPs do, which greatly limits the application of Mn porphyrins *in vivo*.

Received: June 12, 2012
Published: May 6, 2013

INTRODUCTION

While the general and biomimetic chemistry of the *para* isomer FeTE-2-PyP^{5+} (the first metalloporphyrin-based SOD mimic characterized) has been extensively explored, the data on the redox and coordination chemistry of its *meta* and *ortho* analogues and longer alkyl chain derivatives have been considerably neglected. On the redox modulation front, *in vivo* studies on Fe porphyrins as SOD mimics and/or peroxynitrite decomposition catalysts have been limited to compounds from our own laboratory, and to FP-15, INO-4885, and WW-85.[1−8] We have explored a series of anionic and cationic Mn and Fe porphyrins a decade ago and established the structure−activity relationship between their metal-centered reduction potential for (X)M^{III}P/(X)M^{II}P redox couple (M = metal, X = H_2O or OH^-), $E_{1/2}$, and ability to catalyze $O_2^{\bullet-}$ dismutation, $k_{cat}(O_2^{\bullet-})$.[6,8−11] We have further shown that in addition to these thermodynamic parameters, as it is with natural SODs, electrostatics plays a major role in modulating the kinetic parameter k_{cat}.[12,13] Although both Fe and Mn cationic *N*-alkylpyridylporphyrins are potent SOD mimics, as inferred by their k_{cat} values, earlier side-by-side *in vivo* studies at doses of ∼20 μM revealed that only Mn porphyrins offered the highest protection to SOD-deficient *E. coli*, while Fe porphyrins were toxic.[8] Therefore, in an attempt to avoid any possible toxicity arising from Fe-driven Fenton chemistry, we have since explored predominantly Mn porphyrins.[6,10,11,14−16]

Recent dose-dependence studies on SOD-deficient *E. coli*, however, suggested that Fe porphyrins may be efficacious at concentrations orders of magnitude lower than Mn porphyrins. This prompted us to undertake a systematic comparison of Fe versus Mn porphyrin-based compounds. Specifically for this work, we synthesized and fully characterized a series of *ortho* and *meta* Fe(III) *N*-alkylpyridylporphyrins (Figure 1), which were used to probe the effect of electron-deficiency of Fe and Mn sites upon their dismuting ability, $k_{cat}(O_2^{\bullet-})$, metal(III)/metal(II) reduction potential, $E_{1/2}$, compound lipophilicity, and stability toward oxidative degradation. Finally we compared side-by-side the ability of Fe and Mn complexes to protect SOD-deficient *E. coli* against endogenously generated $O_2^{\bullet-}$, and evaluated their systemic toxicity to mice.

EXPERIMENTAL SECTION

General. *Meso*-tetrakis(2-*N*-pyridyl)porphyrin (H_2T-2-PyP) and *meso*-tetrakis(3-*N*-pyridyl)porphyrin (H_2T-3-PyP) were purchased from Frontier Scientific. Ethyl *p*-toluenesulfonate (98%) and methyl *p*-toluenesulfonate were from Sigma-Aldrich. *n*-Butyl *p*-toluenesulfonate, *n*-hexyl *p*-toluenesulfonate, *n*-octyl *p*-toluenesulfonate, and methyltri-*n*-octylammonium chloride (>95%) were from TCI America. $MnCl_2 \times 4H_2O$ (99.7%) was supplied by J. T. Baker, $FeCl_2$ (98%) was from Aldrich, and NH_4PF_6 (99.99%) was from GFS chemicals. Anhydrous diethyl ether and acetone were from EMD chemicals, while dichloromethane, chloroform, acetonitrile, EDTA, and KNO_3 were purchased from Mallinckrodt. Anhydrous *N*,*N*-dimethylformamide (DMF) of 99.8% purity (kept over 4-Å molecular sieves) and plastic-backed silica gel TLC plates (Z122777-25EA) were from Sigma-Aldrich. Xanthine, equine ferricytochrome *c* (Lot 7752), and (+)-sodium L-ascorbate (>98%) were from Sigma, whereas xanthine oxidase was prepared by R. Wiley.[9] $FeSO_4$, $MnSO_4$, and sodium citrate was from Sigma Aldrich. To prepare Mn and Fe citrates, the Na citrate was added to a 10 mM stock solution of $FeSO_4$ or $MnSO_4$. Fresh metal citrate solution was prepared for each experiment.

All chemicals were used as received without further purification.

Synthesis. The general synthetic procedure for *meso*-tetra(*N*-alkylpyridinium-2 or 3-yl)porphyrins and their iron complexes is shown in Figure 2. Method A was used for the synthesis of all *meta* and shorter-chain *ortho* analogues, while for longer-chain *n*-hexyl and *n*-octyl *ortho* species, method B was applied.

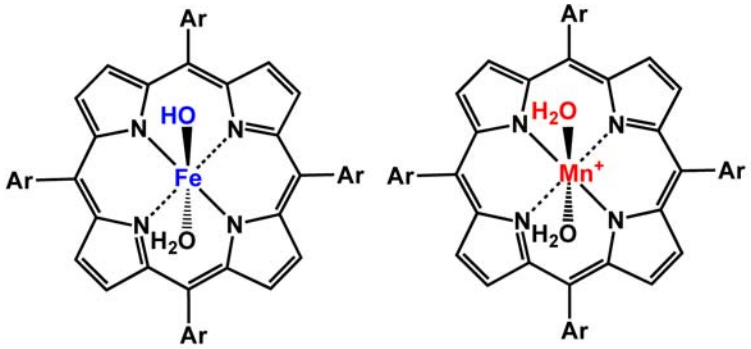

Alkyl side chain on Ar	Methyl	Ethyl	n-Butyl	n-Hexyl	n-Octyl
Ortho(2) Isomers, Ar =					
Meta(3) Isomers, Ar =					

Figure 1. Structures of *ortho* and *meta* isomeric Fe(III) and Mn(III) *meso*-tetrakis *N*-alkylpyridylporphyrins. Axial ligands indicated on the schemes are not related to the complexes isolated in solid state but to the species present at physiological pH in aqueous systems (see Protonation Equilibria section).

dx.doi.org/10.1021/ic3012519 | *Inorg. Chem.* 2013, 52, 5677−5691

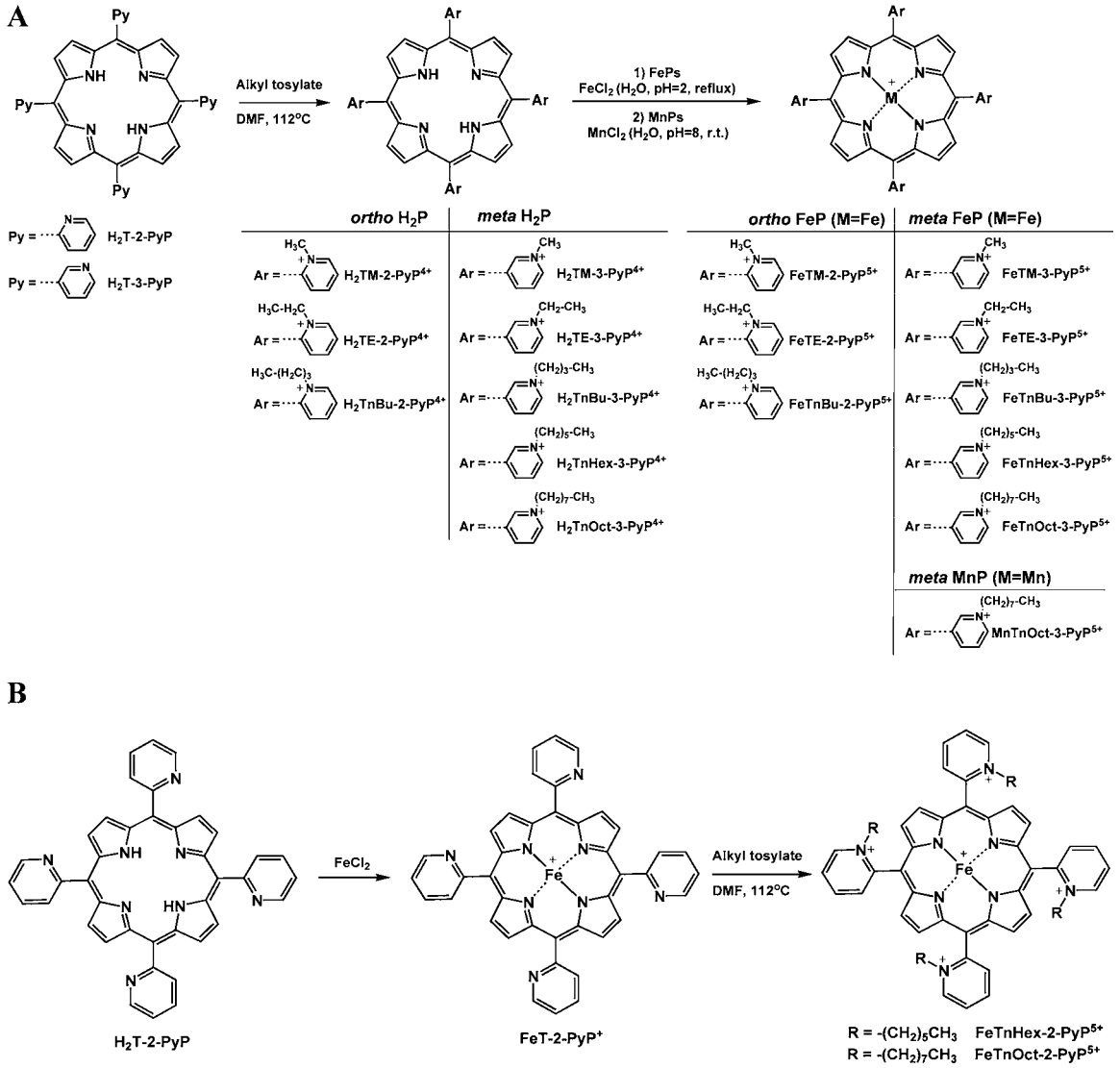

Figure 2. The synthesis of metalloporphyrins. In method A, the ligand was first alkylated and then metalated. The procedure was adapted from that previously described for the methyl analogue.[8] In method B, the ligand was first metalated and then alkylated (described in brief under Synthesis). After alkylation was completed, the rest of the workup procedure was analogous to that described previously.[8]

Method A. Synthesis of *meta* Fe Porphyrins. *Alkylation.* The synthesis, isolation, purification, and characterization of H_2TM-3-PyPCl_4, H_2TE-3-PyPCl_4, H_2TnBu-3-PyPCl_4 and H_2TnHex-3-PyPCl_4 were performed as described earlier.[6,8,17] H_2TnOct-3-PyPCl_4: H_2T-3-PyP (300 mg; 0.485 mmol) was dissolved in 25 mL of DMF at 112 °C, preheated for 10 min, and to the resulting solution 25 g (0.088 mol) of *n*-octyl *p*-toluenesulfonate was added. The course of *N*-octylation was followed by thin-layer chromatography (TLC) on silica gel plates using acetonitrile/$KNO_{3(sat)}$/water = 8:1:1 as the mobile phase. The reaction was completed within 5 h. Porphyrin was precipitated from the reaction mixture by diethyl ether, filtrated, and washed with diethyl ether (5 × 50 mL). It was then dissolved in methanol and purified as described previously for their shorter alkyl-chain analogues.[31,37,43] Yield (calculated based on formulation given by elemental analysis): 650 mg (96%). Metalation: The pH of an aqueous solution of H_2Talkyl-3-PyPCl_4 (~2 mM) was adjusted to 2 (with 1 M HCl), and a 40-fold molar excess $FeCl_2$ was added into the solution and stirred at reflux. The course of metalation was followed on silica gel TLC plates using acetonitrile/$KNO_{3(sat)}$/water = 8:1:1 as a mobile phase (pH = 2, adjusted by 1 M HCl). Additionally, the loss of metal-free porphyrin fluorescence under UV light at ~350 nm was determined. The metalation proceeded relatively fast with *meta* series of porphyrins: after 5 h the reaction was completed. The solution was filtered first through coarse then through fine filter papers. The Fe porphyrin was precipitated as the PF_6^- salt with saturated aqueous solution of NH_4PF_6. The precipitate was thoroughly washed with diethyl ether. The dried precipitate was then dissolved in acetone, filtered, and precipitated as the chloride salt with saturated acetone solution of methyl-tri-*n*-octylammonium chloride. The precipitate was washed with acetone and dissolved in water. The whole precipitation procedure was repeated once again to ensure high purity of preparation. The *meta* Fe porphyrins were isolated in quantitative yields.

Synthesis of *ortho* Fe Porphyrins. *Alkylation.* The synthesis, isolation, purification, and characterization of metal-free H_2TM-2-PyPCl_4, H_2TE-2-PyPCl_4, and H_2TnBu-2-PyPCl_4 were earlier described.[6,8] ***Metalation:*** The metalation and purification of *ortho* isomeric porphyrins were similar to their *meta* analogues except that $FeCl_2$ was added in a 100-fold molar excess. The metalation was slower due to the steric hindrance of the vertically stuck alkyl chains.

Method B. Fe(III) *meso*-tetrakis(2-pyridyl)porphyrin, FeT-2-PyP$^+$ (Figure 2B). The 150 mg of H_2T-2-PyP was dissolved in ~20 mL of chloroform and 3 mL of methanol, and preheated for about 10 min to fully dissolve the compound. Then, the 150 mg of $FeCl_2$ was dissolved in 10 mL of warm ethanol and added to the porphyrin mixture. The course of metalation was followed on silica gel TLC plates using 1:5 methanol/chloroform mixture as a mobile phase. The reaction was completed in

dx.doi.org/10.1021/ic3012519 | *Inorg. Chem.* 2013, 52, 5677−5691

an hour (no fluorescence observed on the TLC plate). The solvent was then evaporated to ~5 mL volume. Ammonium hydroxide was subsequently added to the reaction mixture to precipitate the porphyrin. The precipitate was then filtered through fritted disc and washed with water until neutral pH. The precipitate was washed to dryness with diethyl ether and dissolved on fritted disc with dichloromethane. A purple solid was obtained after solvent evaporation. Yield was 165 mg. FeTnHex-2-PyPCl$_5$: 50 mg (0.071 mmol) of Fe(III) *meso*-tetrakis(2-*N*-pyridyl)porphyrin was dissolved in 3 mL of DMF at 112 °C and preheated for 10 min under nitrogen. To the resulting solution, 4.2 mL (0.018 mol) of *n*-hexyl *p*-toluenesulfonate was added. The course of *N*-hexylation was followed by thin-layer chromatography on silica gel TLC plates using acetonitrile/KNO$_{3(sat)}$/water = 8:1:1 as a mobile phase (pH = 2, adjusted by 1 M HCl). The reaction was completed after a day of stirring at 112 °C. The isolation and purification of FeTnHex-2-PyPCl$_5$ were done as described for *meta* Fe porphyrins via method A. FeTnOct-2-PyPCl$_5$: The synthesis and purification were similar to those described for FeTnHex-2-PyPCl$_5$. The yields of FeTnHex-2-PyPCl$_5$ and FeTnOct-2-PyPCl$_5$ were quantitative.

Synthesis of Mn Porphyrins. MnTM-2-PyPCl$_5$, MnTE-2-PyPCl$_5$, MnTnPr-2-PyPCl$_5$, MnTnBu-2-PyPCl$_5$, MnTnHex-2-PyPCl$_5$, MnTnHep-2-PyPCl$_5$, MnTnOct-2-PyPCl$_5$, MnTM-3-PyPCl$_5$, MnTE-3-PyPCl$_5$, MnTnBu-3-PyPCl$_5$, MnTnHex-3-PyPCl$_5$: Synthesis of these Mn porphyrins was performed as described elsewhere.[6,8,17] MnTnOct-3-PyPCl$_5$: 150 mg of H$_2$TnOct-3-PyPCl$_4$ (0.124 mmol) was dissolved in 60 mL of water and the pH of the resulting solution was adjusted to 11.5. A 20-fold excess MnCl$_2$ (2.47 mmol, 0.49 g) was added into the solution at 25 °C while stirring, resulting in a pH drop to ~8.0. The course of metalation was followed on silica gel TLC plates using acetonitrile/KNO$_{3(sat)}$/water = 8:1:1 as a mobile phase. After 12 h of stirring, the reaction was worked-up by filtration and PF_6^-/Cl^- sequential precipitation procedures: the isolation and purification of the MnTnOct-3-PyPCl$_5$ were done as described for the *meta* Fe porphyrins (see above). The isolated yield was quantitative.

Elemental Analysis. Elemental analyses of H$_2$TnOct-3-PyPCl$_4$ and metal complexes were performed by Atlantic MicroLab (Norcross, GA, USA). All analyses were done in duplicates. Formulations accounting for 9−13 hydration waters are consistent with related MnTE-2-PyPCl$_5$·11H$_2$O sample isolated under similar conditions.[18]

FeTE-3-PyPCl$_5$·11H$_2$O: Anal. Calcd for $C_{48}H_{66}Cl_5FeN_8O_{11}$: H, 5.71; C, 49.52; N, 9.63; Cl, 15.23%. Found: H, 5.51; C, 49.35; N, 9.56; Cl, 14.87%.

FeTnBut-2-PyPCl$_5$·11H$_2$O: Anal. Calcd for $C_{56}H_{82}Cl_5FeN_8O_{11}$: H, 6.48; C, 52.69; N, 8.78; Cl, 13.89%. Found: H, 6.43; C, 52.72; N, 8.85; Cl, 13.56%.

FeTnBut-3-PyPCl$_5$·10H$_2$O: Anal. Calcd for $C_{56}H_{80}Cl_5FeN_8O_{10}$: H, 6.41; C, 53.45; N, 8.9; Cl, 14.09%. Found: H, 6.38; C, 53.22; N, 9.01; Cl, 13.8%.

FeTnHex-2-PyPCl$_5$·11H$_2$O: Anal. Calcd for $C_{64}H_{116}Cl_5FeN_8O_{11}$: H, 7.11; C, 55.36; N, 8.07; Cl, 12.77%. Found: H, 6.81; C, 55.27; N, 8.22; Cl, 12.37%.

FeTnHex-3-PyPCl$_5$·9H$_2$O: Anal. Calcd for $C_{64}H_{94}Cl_5FeN_8O_9$: H, 7.00; C, 56.83; N, 8.28; Cl, 13.12%. Found: H, 6.79; C, 56.67; N, 8.35; Cl, 12.76%.

FeTnOct-2-PyPCl$_5$·13H$_2$O: Anal. Calcd for $C_{72}H_{118}Cl_5FeN_8O_{13}$: H, 7.74; C, 56.27; N, 7.29; Cl, 11.53%. Found: H, 7.01; C, 55.81; N, 7.32; Cl, 11.32%.

FeTnOct-3-PyPCl$_5$·10H$_2$O: Anal. Calcd for $C_{72}H_{112}Cl_5FeN_8O_{10}$: H, 7.61; C, 58.32; N, 7.56; Cl, 11.95%. Found: H, 7.40; C, 58.00; N, 7.54; Cl, 11.58%.

H$_2$TnOct-3-PyPCl$_4$ 10H$_2$O: Anal. Calcd for $C_{72}H_{114}Cl_4N_8O_{10}$: H, 8.25; C, 62.06; N, 8.04; Cl, 10.18%. Found: H, 7.96; C, 62.05; N, 8.04; Cl, 10.4%.

MnTnOct-3-PyPCl$_5$·10H$_2$O: Anal. Calcd for $C_{72}H_{112}Cl_5MnN_8O_{10}$: H, 7.62; C, 58.36; N, 7.56; Cl, 11.96%. Found: H, 7.43; C, 57.99; N, 7.55; Cl, 11.87%.

UV/vis Spectroscopy. UV/vis spectra were recorded in 0.01 M HCl at room temperature on a UV-2550 PC Shimadzu spectrophotometer with 0.5 nm resolution using a 1 cm quartz cuvette. The data at pH 2 relate to diaqua Fe porphyrins (Table 1).

Table 1. The Spectral Properties of H$_2$TnOct-3-PyPCl$_4$ and Metal Complexes

Porphyrin	λ_{max} nm (log ε)[a]
FeTM-2-PyPCl$_5$	395.0 (5.11), 500.0 (4.15), 610.0 (3.91)[b]
FeTM-3-PyPCl$_5$	397.8 (5.01)[b]
FeTE-2-PyPCl$_5$	396.8 (5.16)[b]
FeTE-3-PyPCl$_5$	262.2 (4.47), 333.3 (4.52), 396.4 (5.11), 509.2 (4.05)
FeTnBu-2-PyPCl$_5$	263.0 (4.44), 395.6 (5.03), 500.7 (4.03), 616.0 (3.90)
FeTnBu-3-PyPCl$_5$	262.5 (4.48), 333.5 (4.53), 396.8 (5.10), 506.6 (4.07)
FeTnHex-2-PyPCl$_5$	262.6 (4.47), 395.7 (5.06), 501.0 (4.08), 615.1 (3.95)
FeTnHex-3-PyPCl$_5$	263.3 (4.47), 334.0 (4.51), 397.4 (5.06), 506.8 (4.05)
FeTnOct-2-PyPCl$_5$	263.1 (4.49), 415.0 (5.03), 500.2 (4.11), 616.1 (3.95)
FeTnOct-3-PyPCl$_5$	263.0 (4.47), 333.7 (4.47), 397.5 (5.08), 507.7 (4.06), 577.6 (3.88)
H$_2$TnOct-3-PyPCl$_4$	263.1 (4.41), 417.8 (5.55), 514.2 (4.29), 581.6 (3.85), 636.1 (3.01)[c]
MnTnOct-3-PyPCl$_5$	215.2 (4.77), 261.6 (4.58), 373.9 (4.72), 395.0 (4.69), 460.0 (5.18), 501.6 (3.88), 557.8 (4.16), 675.1 (3.37), 765.6 (3.40)[c]

[a]Spectra were measured in 0.01 M HCl at room temperature, unless noted otherwise. Thus, all metalloporphyrins have two H$_2$O molecules as axial ligands. Molar absorption coefficients (M^{-1} cm^{-1}) were determined within 5% errors considering the formulation given by elemental analysis. λ_{max} (nm) were determined with errors inside ±0.5 nm. [b]Data are taken from ref 6. [c]Spectra were taken in water at room temperature.

Electrospray-Ionization Mass Spectrometry. Electrospray ionization mass spectrometric (ESI-MS) analyses were performed as described elsewhere,[17,19,20] on an Applied Biosystems MDS Sciex 3200 Q Trap LC/MS/MS spectrometer at Duke Comprehensive Cancer Center, Shared Resource PK Laboratories. Samples of ~1 μM concentrations were prepared in acetonitrile/H$_2$O mixture (1:1, v/v) containing 0.01% v/v heptafluorobutyric acid and infused for 1 min at 10 μL/min into the spectrometer (curtain gas 20 V, ion spray voltage 3500 V, ion source 30 V, t = 300 °C, declustering potential 20 V, entrance potential 1 V, collision energy 5 V, gas N$_2$). Under given conditions, in the presence of ion-pairing heptafluorobutyrate anion ($HFBA^-$) no fragmentation is observed; the data relate to species originally present in solutions. The absence of peaks associated with partially alkylated and nonmetalated species unambiguously indicates the purity of the sample. No peaks associated with species bearing axial hydroxo ligands were observed in mass spectra in the presence of heptafluorobutyric acid. Data are summarized in Table 2.

Redox Property of Metal Site and Protonation Equilibria of Axial Waters. *Electrochemistry.* Cyclic voltammetry measurements were performed in a glass cell under argon atmosphere, using a CH Instruments model 600 voltammetric analyzer, as described previously.[21,22] Stock solutions of Fe porphyrins were prepared by dissolving solid substances in deionized water. Working solutions of ~0.2 mM Fe porphyrins were prepared immediately before measurements, either in 0.01 M HCl (pH = 2) or in 0.05 M phosphate buffer (pH = 7.8). The supporting electrolyte in all measurements was 0.1 M NaCl. The pH of working solutions was determined on a Denver Instrument model 250 pH-meter using a glass electrode calibrated with the standard buffers (pH 4.00, 7.00, and 10.00). The concentrations of Fe porphyrins were determined spectrophotometrically. All potentials are reported vs the normal hydrogen electrode (NHE), using the known potential of $(H_2O)_2$MnTE-2-PyP^{5+}, $E_{1/2}$ = +228 mV vs NHE, as a reference.[17,20,23] No μ-oxo dimers were observed under given pH and concentration conditions as well as at pH 12. The Spiro's group[24] observed μ-oxo dimers with (OH)(H$_2$O)FeTM-2-PyP^{4+} but with 1 mM porphyrin solutions and at pH 9 and 12. The $E_{1/2}$ of $(H_2O)_2$MnTE-2-PyP^{5+} was determined before and after each series of measurements.

dx.doi.org/10.1021/ic3012519 | *Inorg. Chem.* 2013, 52, 5677−5691

Table 2. Electrospray Ionization Mass Spectrometry (ESI-MS) Data for Fe Porphyrins[b]

species[a]	m/z [found (calculated)]						
	FeTE-3-PyP^{5+}	FeTnBu-2-PyP^{5+}	FeTnBu-3-PyP^{5+}	FeTnHex-2-PyP^{5+}	FeTnHex-3-PyP^{5+}	FeTnOct-2-PyP^{5+}	FeTnOct-3-PyP^{5+}
$[FeP^{5+} + HFBA^-]^{4+}/4$	250.4 (250.3)	278.5 (278.4)	278.4 (278.4)	306.5 (306.4)	306.6 (306.4)	334.7 (334.4)	334.5 (334.4)
$[FeP^{5+} + 2HFBA^-]^{3+}/3$	404.8 (404.8)	442.3 (442.1)	442.1 (442.1)	497.5 (497.5)	479.5 (479.5)	517 (516.9)	516.8 (516.9)
$[FeP^{5+} + 3HFBA^-]^{2+}/2$	713.5 (713.6)	769.5 (769.7)	769.5 (769.7)	825.6 (825.7)	825.5 (825.7)	881.5 (881.8)	881.5 (881.8)

[a] ~1 μM solution of porphyrins and metalloporphyrins in 1:1 v/v acetonitrile/H_2O (containing 0.01% v/v heptafluorobutyric acid (HFBA)) mixture, 20 V cone voltage. [b] In the presence of heptafluorobutyric acid, in the solvent mixture no monohydroxo (OH)(H_2O)FePs species was detected.

Table 3. Electrospray Ionization Mass Spectrometry (ESI-MS) Data for H_2TnOct-3-PyP^{4+} and MnTnOct-3-PyP^{5+}[a]

species	m/z [found (calculated)]	
	H_2TnOct-3-PyP^{4+}	MnTnOct-3-PyP^{5+}
$[P^{n+} + HFBA^-]^{(n-1)+}/(n-1)$	428.1 (427.9)	334.3 (334.2)
$[P^{n+} + 2HFBA^-]^{(n-2)+}/(n-2)$	748.3 (748.4)	516.7 (516.5)
$[P^{n+} + 3HFBA^-]^{(n-3)+}/(n-3)$		881.0 (881.3)
$P^{n+}/4$	267.9 (267.7)	
$[P^{4+} - H^+]^{3+}/3$	356.6 (356.6)	

[a] ~1 μM solution of porphyrins and metalloporphyrins in 1: 1 v/v acetonitrile/H_2O (containing 0.01% v/v heptafluorobutyric acid (HFBA)) mixture, 20 V cone voltage.

Protonation Equilibria. The pK_a values of the axial waters for MnPs have been reported previously.[25,26] The existence of diaqua (i.e., fully protonated) species of either *ortho*, *meta*, or *para* *N*-methylpyridyl Fe(III) porphyrins at pH = 2 has been documented in the literature,[8,24,25,27−31] as determined by spectroscopic and electrochemical methods. The relationships between pK_a values for Fe +3 and Fe +2 oxidation states of the metal sites of these isomers have been documented as well. Kobayashi et al. reported values of pK_{a1} = 5.3−5.9 and pK_{a2} = 10.1−12.3 for $(H_2O)_2Fe^{III}$TM-2(3 and 4)-PyP^{5+} and pK'_{a1} = 10.8−12.2 for $(H_2O)Fe^{II}$TM-2(3 and 4)-PyP^{4+}.[29,30] The data indicate significantly decreased acidity of Fe^{II}Ps compared to Fe^{III}Ps, due to a large decrease in electron-deficiency upon Fe^{III}P reduction.

Consequently, in the region pH = 2−8, any shift in the redox potential depends solely on the deprotonation of Fe^{III}P, assuming that the differences in the pyridyl substituents should not affect the established relationships significantly (i.e., $K_{a1} \gg K_{a2}$ and $K_{a1} \gg K'_{a1}$), already demonstrated for the corresponding MnP isomers.[25,26] Specifically, the lengthening of the alkyl chain does not affect axial protonation equilibria: the pK_{a1} and pK_{a2} for Mn(III) methyl to *n*-octyl *ortho* analogues differ insignificantly, by only 0.5 and 0.3 units, respectively.[25] Therefore, a simple expression given in eq 1 could be applied to calculate the pK_{a1} values (Table 4) for other Fe^{III}P analogues described in this work:

$$pK_a = 7.8 - \Delta E/0.059 \quad (1)$$

where $\Delta E = E_{1/2}$ (pH = 2) − $E_{1/2}$ (pH = 7.8).

Stability toward Oxidative Degradation. The stability of metalloporphyrins toward ascorbate-mediated oxidative degradation with regard to alkyl chain length (ethyl vs hexyl), its position on the pyridyl ring (*ortho vs meta*), and the type of metal center (Fe vs Mn) was explored. Metalloporphyrins catalyze the oxidation of ascorbate and thiols.[20,32] Herein we explored their reactivity toward ascorbate (Figure 3, process I). The subsequent peroxide formation degrades porphyrin (Figure 3, process II).[20,33,34] The stability of porphyrins toward H_2O_2 was studied also, and data are in agreement with those previously reported.[8] The conditions were 6 μM metalloporphyrin, 0.42 mM sodium ascorbate at pH 7.8 maintained with 0.05 M Tris buffer.

Lipophilicity. We have shown that both the TLC retention factor, R_f, and the partition between *n*-octanol and water, log P_{OW}, are equally valid parameters in assessing Mn porphyrin lipophilicity.[6,17] Herein we assessed lipophilicity via R_f, in acetonitrile/$KNO_{3(sat)}$/water = 8:1:1 as previously described.[17] The R_f value for Fe and Mn porphyrins was determined at pH 2, adjusted with the addition of 1 M HCl solution to the chromatographic solvent system. At this pH, the predominant species of either Fe or Mn porphyrins is diaqua, which is consistent with the same profile of the distribution of atropoisomers on the TLC plate both for Fe and Mn porphyrins. Because of the different protonation equilibria of Fe vs Mn porphyrins, the partition between water and *n*-octanol, log P_{OW}, was not assessed, as that would not allow the comparison of the same FeP and MnP species. The data are summarized in Table 5.

SOD-like Activity of Metalloporphyrins. SOD activity was examined using the cytochrome *c* (cyt *c*) assay.[20,22,23] The experiments were conducted at room temperature in 0.05 M potassium phosphate buffer, pH 7.8, and 0.1 mM EDTA, as reported.[20,22,23] Data are summarized in Table 4.

Superoxide-Specific Biological Model - Aerobic Growth of SOD-Deficient *E. coli*. *E. coli* mutants lacking the two cytosolic

Table 4. The Reduction Potentials $E_{1/2}$ for M^{III}/M^{II} Redox Couple (M = Fe, Mn), Deprotonation Constant, pK_{a1} for the Axial Water of $(H_2O)_2$FePs, and SOD Activity, Given As log $k_{cat}(O_2^{\bullet-})$

compound		$(H_2O)_2FeP^{5+}$		$(OH)(H_2O)FeP^{4+}$		$(H_2O)_2MnP^{5+}$	
		$E_{1/2}$ (pH = 2)[a]	pK_{a1}[b]	$E_{1/2}$ (pH = 7.8)[a]	log $k_{cat}(O_2^{\bullet-})$	$E_{1/2}$ (pH = 7.8)[a,c]	log $k_{cat}(O_2^{\bullet-})$[c]
ortho isomers	methyl	0.381	5.02	0.217	7.89	0.220	7.79
	ethyl	0.369	5.12	0.211	8.05	0.228	7.76
	n-butyl	0.348	5.95	0.239	7.82	0.254	7.25
	n-hexyl	0.370	5.75	0.249	7.53	0.314	7.48
	n-octyl	0.406	5.34	0.261	7.09	0.367	7.71
meta isomers	methyl	0.232	5.66	0.106	6.99	0.052	6.61
	ethyl	0.229	5.68	0.104	6.98	0.054	6.65
	n-butyl	0.232	5.63	0.104	6.99	0.064	6.69
	n-hexyl	0.230	5.77	0.110	6.86	0.066	6.64
	n-octyl	0.236	5.95	0.127	6.93	0.074	6.53

[a] Redox potentials are given in volts vs NHE. [b] Deprotonation constants are estimated according to eq 1. [c] Redox potentials and rate constants (in M^{-1} s^{-1}) are from refs 6 and 11 except for $(H_2O)_2$MnTnOct-3-PyP^{5+}, this work.

dx.doi.org/10.1021/ic3012519 | *Inorg. Chem.* 2013, 52, 5677−5691

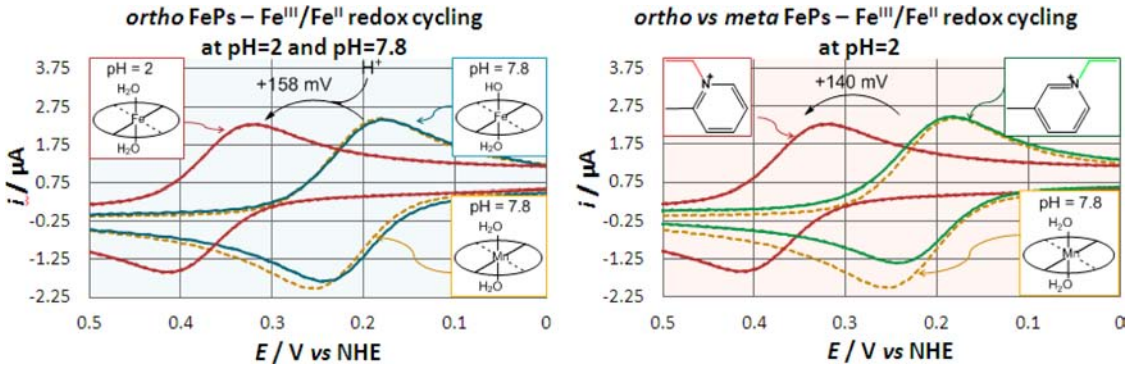

Figure 3. The electrochemistry of Fe and Mn porphyrins as exemplified with ethyl analogues. The cyclic voltammetry of Fe porphyrins (0.2 mM) was performed at pH = 2 and at pH = 7.8 where different species exist, $(H_2O)_2$FeTE-2(or 3)-PyP^{5+} and (H_2O)(OH)FeTE-2(or 3)-PyP^{4+}, respectively. The increase of pH from 2 to 7.8, associated with the change in a type of species present, resulted in a shift of $E_{1/2}$ from +369 to +211 mV (left panel). Under both pH conditions the same diaqua Mn porphyrin ($(H_2O)_2$MnTE-2-PyP^{5+}) exists.[8] The shift of $E_{1/2}$ from +369 with $(H_2O)_2$FeTE-2-PyP^{5+} to +228 with $(H_2O)_2$MnTE-2-PyP^{5+} reflects much higher electron-deficiency of Fe than the Mn site. Similar to Mn porphyrins, the $E_{1/2}$ of *ortho* Fe porphyrins is higher than that of *meta* isomers (right panel) due to stronger electron-withdrawing properties of the pyridyl nitrogens situated closer to the metal center. $(H_2O)_2$MnTE-2-PyP^{5+} was herein used as a standard. No μ-oxo dimers were observed under given experimental conditions (0.2 mM concentration at pH = 2 and 7.8). No axial ligands are specified in the figure titles, as FeP species studied bear different axial ligands.

Table 5. Lipophilicity of Mn and Fe Porphyrin-Based SOD Mimics Expressed in Terms of R_f Values Taken in Acetonitrile/KNO$_{3(sat)}$/Water = 8:1:1 Solvent System at pH 2[a]

metalloporphyrin		R_f	
		$(H_2O)_2$FeP^{5+}	$(H_2O)_2$MnP^{5+}
ortho isomers	methyl	0.131	0.125
	ethyl	0.186	0.156
	n-butyl	0.443	0.394
	n-hexyl	0.597	0.600
	n-octyl	0.640	0.644
meta isomers	methyl	0.160	0.125
	ethyl	0.246	0.188
	n-butyl	0.554	0.538
	n-hexyl	0.646	0.631
	n-octyl	0.674	0.656

[a]The R_f values relate to the diaqua Fe and diaqua Mn porphyrin species.

superoxide dismutases (FeSOD and MnSOD, *sodA*$^-$*sodB*$^-$) suffer phenotypic deficiencies including poor aerobic growth[35] and auxotrophies for branched-chain,[36] aromatic,[37] and sulfur-containing amino acids.[38] The failure of the *sodA*$^-$*sodB*$^-$ mutants to grow aerobically in the absence of the listed amino acids can be relieved by compounds scavenging superoxide. Therefore, aerobic growth of *sodA*$^-$*sodB*$^-$ *E. coli* in a restricted, five amino-acid (5AA) medium can be used to assess the capacity of SOD mimics to substitute for the natural enzymes. The 5AA medium consisted of M9 salts supplemented with filter-sterilized L-leucine, L-threonine, L-proline, L-arginine, and L-histidine at a final concentration of 0.5 mM each, 0.2% glucose and 3 mg/L of pantothenic acid and thiamine. M9 salts were prepared by autoclaving 0.6 g of Na_2HPO_4, 0.3 g of KH_2PO_4, 0.05 g of NaCl, and 0.1 g of NH_4Cl per liter in distilled water. After cooling, separately autoclaved solutions of $MgSO_4$ and $CaCl_2$ were added to a final concentration of 1.0 mM. Growth of the SOD-proficient AB1157 (*F-thr-1; leuB6; proA2; his-4; thi-1; argE2; lacY1; galK2; rpsL; supE44; ara-14; xyl-15; mtl-1; tsx-33*) and the SOD-deficient (*sodA*$^-$*sodB*$^-$) JI132 (same as AB1157 plus (*sodA::mudPR13*)25 (*sodB-kan*)1-Δ2) *E. coli* strains in 5AA medium was done as already described.[20] Both strains were obtained from J. A. Imlay.[39] The effect of the compounds was tested in parallel on parental and SOD-deficient strains with different genetic background: GC4468 = parental strain; SOD-deficient, QC1799 = GC4468 Δ*sod*A3, Δ*sod*B-kan[40] (D. Touati, Institute Jacques Monod, CNRS, Universite Paris, France). No significant differences between the two sets of strains were observed.

The effect of (OH)(H_2O)FePs (0.01−25 μM) on the growth of the SOD-deficient mutant in 5AA medium was compared to the effect of optimal 20 μM Mn ethyl analogues *ortho* $(H_2O)_2$MnTE-2-PyP^{5+} and *meta* $(H_2O)_2$MnTE-3-PyP^{5+}. For comparison, the effect of different Mn and Fe salts was studies. The corresponding anions had no effect on cell growth: citrate, sulfate, and chloride salts of Fe and Mn had identical effect.

At different time points, the cells were harvested, rapidly washed with cold buffered saline, and disrupted by French pressing. Cytosolic fractions were isolated as described earlier,[41] and the content of metalloporphyrins was determined by UV/vis spectroscopy. Aliquots of the growth media were analyzed at same time points.

Mouse Study. All animal procedures were conducted in accordance with IUCAC guidelines and approval from Duke University Medical Center, as described in the Guide for Care and Use of Laboratory Animals published by the National Institutes of Health (publication #NIH 85-23, revised 1985). Animals were housed on a 12 h light cycle (lights on at 6:00 a.m.) with standard laboratory diets and water available ad libitum. 8−10 weeks old male C57BL/6J mice were used for studies.

Both Fe- and Mn porphyrins were administered by intraperitoneal (i.p.) injection. Maximal tolerable doses (MTDs) were considered those which caused mild and transient toxicity manifested by quietness, lethargy, and reluctance to ambulate. Then, doses of 10 mg/kg of (OH)(H_2O)FeTE-2-PyP^{4+}, 10 mg/kg of $(H_2O)_2$MnTE-2-PyP^{5+}, 5 mg/kg (OH)(H_2O)FeTnHex-2-PyP^{4+}, and 1 mg/kg of $(H_2O)_2$-MnTnHex-2-PyP^{5+} were selected for the toxicity study. The compounds were administered i.p. twice per day for one week. Animal behavior, weight and performance on rotarod were followed for one week as described previously.[23]

The effect of porphyrins on arterial blood pressure was also assessed through right femoral artery in isoflurane anesthetized mice. After 15 min of baseline recording, 10 mg/kg porphyrin was slowly infused in 5 min and arterial blood pressure was continuously monitored for 30 min. (Procedure: Mice were anesthetized with 5% isoflurane in 30% oxygen balanced with nitrogen and intubated. Both lungs were mechanically controlled by a rodent ventilator. Body temperature was controlled at 37 °C. Both right femoral artery and vein were cannulated by PE-10 tubes for blood pressure measurement and porphyrin slow infusion, respectively.

dx.doi.org/10.1021/ic3012519 | *Inorg. Chem.* 2013, 52, 5677−5691

RESULTS AND DISCUSSION

Redox Property of Metal Site and Protonation Equilibria of Axial Waters of Metalloporphyrins. We have already reported that the major difference between the speciation of Fe and Mn cationic *N*-alkylpyridylporphyrins in aqueous systems at physiological conditions (at pH 7.8) is the presence of axial electron-rich hydroxo ligand with Fe- vs electron-poor axial aqua ligand with Mn porphyrins.[8] All *ortho* and *meta* Fe porphyrins exhibited an acid−base behavior governed by the two proton-transfer equilibria represented by eqs 2 and 3, whose first proton dissociation constants (pK_{a1}) fall in the 5−6 range (Table 4) followed by the second proton dissociation constant (pK_{a2}) of ∼11. The pK_a data for $(H_2O)_2$FeTM-2(or 3 or 4)-PyP^{5+} are in agreement with those previously reported.[8,24,27,29−31] These pK_a sets indicate that all FePs have lost a proton from the coordinated axial water to yield the hydroxo-aqua complex as the major species at pH 7.8. Conversely, the acid−base equilibrium of the Mn analogues described by the same eqs 2 and 3, with pK_{a1} and pK_{a2} values for the $(H_2O)_2$MnTM-2(or 3)-PyP^{5+}[8,25] and $(H_2O)_2$MnTE-2(or 3)-PyP^{5+}[26] in the region of ∼10.5−11.4 (*ortho* isomers) and ∼11.5−13.5 (*meta* isomers), indicate that the Mn porphyrins exist as the diaqua species at pH 7.8.

$$[(H_2O)_2M^{III}P]^{5+} \rightleftharpoons [(OH)(H_2O)M^{III}P]^{4+} + H^+,\ K_{a1} \quad (M = Fe^{III} \text{ or } Mn^{III}) \tag{2}$$

$$[(OH)(H_2O)M^{III}P]^{4+} \rightleftharpoons [(OH)_2M^{III}P]^{3+} + H^+,\ K_{a2} \quad (M = Fe^{III} \text{ or } Mn^{III}) \tag{3}$$

The acidity of the metalloporphyrin axial waters with respect to free water ($pK_w \sim 14$) is increased by ∼8.5 and ∼3 log units upon coordination to the FeP and MnP moieties, respectively. Such a large difference between the pK_{a1} values shows that the axially coordinated water in Fe porphyrins is about 5 log units more acidic than in the corresponding Mn porphyrins. This is in direct contrast with the acidity of simple "free ions", hexaaqua species $[Fe^{III}(H_2O)_6]^{3+}$ ($pK_{a1} \sim 2.2$)[42] and $[Mn^{III}(H_2O)_6]^{3+}$(pK_{a1} ∼ 0.1),[43] which indicates that the Mn^{3+} species is more acidic than the Fe^{3+} complex by ∼2 log units. Thus, substitution of four neutral H_2O ligands in the coordination sphere of free ions by a $[N_4]^{2-}$ coordination system of the porphyrinato ligand (ignoring the charge of the peripheral pyridinium moieties) increases the electronic density around the metal center, which translates into a decrease in the coordinated water acidity; this effect is, however, much more pronounced in the MnP case, where the ligand substitution is followed by an increase of ∼10 log K_{a1} units, whereas the FeP series has pK_{a1} values only ∼3 orders of magnitude greater than those of $[Fe^{III}(H_2O)_6]^{3+}$. On electrostatic grounds, these results suggest that the positive charge on the "$[Fe(H_2O)_2]^{+}$" and "$[Mn(H_2O)_2]^{+}$" moieties in the porphyrin series is considerably more delocalized with MnP, which results in their lower acidity relative to their Fe counterparts. Diaqua and hydroxo-aqua Mn^{III}Ps and Fe^{III}Ps are all high spin species;[6,44] therefore this difference in axial water acidity is not related to a spin state change. Although a full description of aqueous behavior of FeP vs. MnP series based on the metalloporphyrin electronic structure is not yet available, the structural single crystal X-ray data for diaqua complexes of the *para* isomers $(H_2O)_2$FeTM-4-PyP^{5+}[45] and $(H_2O)_2$MnTM-4-PyP^{5+}[46] are consistent with the lower acidity of the MnPs. While the Fe−O_{water} bond length is 2.086 Å, the Mn−O_{water} bond is reasonably longer (2.221 Å), which implies that the axial water molecules in the Fe system are more tightly held as a response to the higher electron-deficiency of the FeP moiety, whose acidity is thus transferred to the coordinated water molecules and deprotonation is favored.

Another major difference in the biology of "free" Fe vs "free" Mn is related to their reduction potentials. Because of a vastly higher reduction potential of "free" Mn^{III}/Mn^{II} (E^o = +1.51 V vs NHE) than of "free" Fe^{III}/Fe^{II} (E^o = +0.77 V vs NHE), Mn cannot be easily oxidized with H_2O_2 to produce $^{\bullet}$OH radical; consequently Mn does not undergo, while Fe is capable of performing "Fenton chemistry" ($Fe^{2+} + H_2O_2 \rightleftharpoons Fe^{3+} + OH^- + {}^{\bullet}OH$).[47] When Mn or Fe binds to SOD protein, the reduction potentials became identical and are within limits of $O_2^{\bullet-}$ oxidation similar to Mn or Fe binding to porphyrin ligand.

With water as axial ligands (at pH = 2),[8] $(H_2O)_2$FeTE-2-PyP^{5+} has much higher $E_{1/2}$ (+369 mV vs NHE) relative to $(H_2O)_2$MnTE-2-PyP^{5+} (+228 mV vs NHE). This is consistent with a stronger electron-deficiency and in turn acidity of the FeP moiety, which is thus more prone to being reduced than the corresponding MnP system. The replacement of an axial aqua with an axial hydroxo ligand in FeP at pH 7.8 shifts the $E_{1/2}$ negatively from +369 to +211 mV vs NHE. Therefore, at pH 7.8 $(H_2O)_2$MnTE-2-PyP^{5+} and $(OH)(H_2O)$FeTE-2-PyP^{4+} have nearly identical $E_{1/2}$ for M^{III}/M^{II} redox couple (+228 and +211 mV vs NHE, respectively) and in turn are equally efficacious SOD mimics (Figure 3, Table 4). The magnitude of the electron donating effect of hydroxo vs aqua ligand is similar to the effect caused by moving the *N*-alkyl chains from *ortho* to *meta* positions at pyridyl rings (Table 4).

Redox Property and SOD-like Activity of Metalloporphyrins. Figures 4 and 5 depict the differences in the relationships between the thermodynamic and kinetic parameters for the $O_2^{\bullet-}$ dismutation (eqs 4 and 5 for Fe porphyrins, eqs 6 and 7 for Mn porphyrins) and the length of the alkyl chains between Fe and Mn porphyrins at pH 7.8.

$$(OH)(H_2O)Fe^{III}P^{4+} + O_2^{\bullet-} \rightleftharpoons (OH)Fe^{II}P^{3+} + O_2 + H_2O \tag{4a}$$

$$(OH)Fe^{II}P^{3+} + H^+ \rightleftharpoons (H_2O)Fe^{II}P^{4+} \tag{4b}$$

$$(OH)(H_2O)Fe^{III}P^{4+} + O_2^{\bullet-} + H^+ \rightleftharpoons (H_2O)Fe^{II}P^{4+} + O_2 + H_2O \tag{4}$$

$$(H_2O)Fe^{II}P^{4+} + O_2^{\bullet-} + 2H^+ \rightleftharpoons (H_2O)Fe^{III}P^{5+} + H_2O_2 \tag{5a}$$

$$(H_2O)Fe^{III}P^{5+} + H_2O \rightleftharpoons (OH)(H_2O)Fe^{III}P^{4+} + H^+ \tag{5b}$$

$$(H_2O)Fe^{II}P^{4+} + O_2^{\bullet-} + H^+ + H_2O \rightleftharpoons (OH)(H_2O)Fe^{III}P^{4+} + H_2O_2 \tag{5}$$

$$(H_2O)_2Mn^{III}P^{5+} + O_2^{\bullet-} \rightleftharpoons (H_2O)_2Mn^{II}P^{4+} + O_2 \tag{6a}$$

$$(H_2O)_2Mn^{II}P^{4+} \rightleftharpoons (H_2O)Mn^{II}P^{4+} + H_2O \tag{6b}$$

$$(H_2O)_2Mn^{III}P^{5+} + O_2^{\bullet-} \rightleftharpoons (H_2O)Mn^{II}P^{4+} + O_2 + H_2O \tag{6}$$

dx.doi.org/10.1021/ic3012519 | Inorg. Chem. 2013, 52, 5677−5691

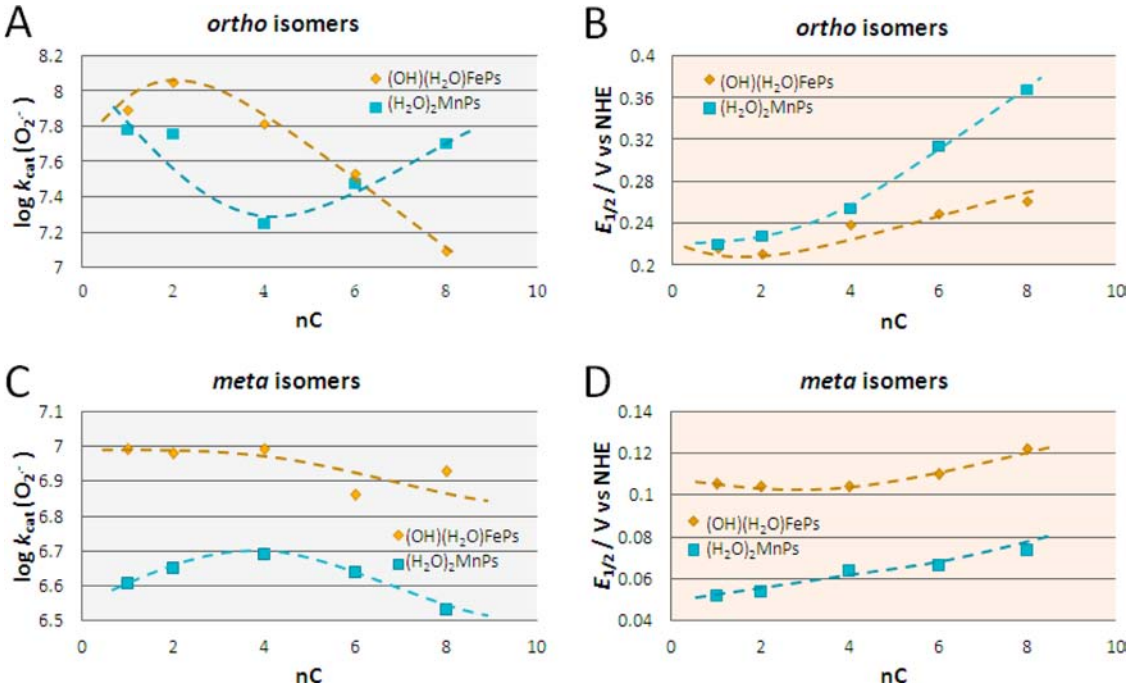

Figure 4. The relationships between each of log k_{cat} ($O_2^{\bullet-}$) (A and C) and $E_{1/2}$ (V vs NHE) (B and D) and the length of the alkyl chains (number of carbon atoms in chains, nC) for *ortho* and *meta* Mn and Fe porphyrins at pH 7.8. Numerical values and the experimental conditions for k_{cat} ($O_2^{\bullet-}$) and $E_{1/2}$ (V vs NHE) are given in Table 5. The effects shown in these plots translate into the $E_{1/2}$ vs log k_{cat} ($O_2^{\bullet-}$) relationships shown in Figure 5. The experimental points are connected to better visualize the trends — no mathematical model was applied.

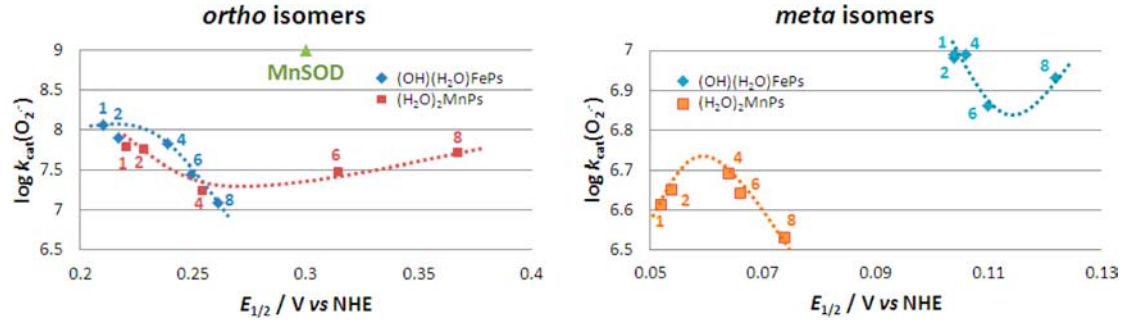

Figure 5. Structure–activity relationships between log $k_{cat}(O_2^{\bullet-})$ and $E_{1/2}$ for M^{III}/M^{II} (M = metal) describe the profound difference between Fe and Mn porphyrins dominated by the differences in the thermodynamic properties and steric and electrostatic factors which all affect porphyrin solvation and approach of anionic superoxide to cationic porphyrin and thus log k_{cat} for the catalysis of $O_2^{\bullet-}$ dismutation. Numbers in the plots correspond to the number of carbon atoms present in each of the *N*-alkyl chains. The experimental points are connected to better visualize the trends — no mathematical model was applied.

$$(H_2O)Mn^{II}P^{4+} + O_2^{\bullet-} + 2H^+ \rightleftharpoons (H_2O)Mn^{III}P^{5+} + H_2O_2 \quad (7a)$$

$$(H_2O)Mn^{III}P^{5+} + H_2O \rightleftharpoons (H_2O)_2Mn^{III}P^{5+} \quad (7b)$$

$$(H_2O)Mn^{II}P^{4+} + O_2^{\bullet-} + 2H^+ + H_2O \rightleftharpoons (H_2O)_2Mn^{III}P^{5+} + H_2O_2 \quad (7)$$

As detailed under the Redox Property of Metal Site and Protonation Equilibria, the differences are the consequence of the vast difference in the electron-deficiency of the metal site, which results in different species present in solution under physiological conditions: (OH)(H_2O)FePs vs (H_2O)$_2$MnP.[8,24,48] The OH^- axial ligand affects both thermodynamics and kinetics of $O_2^{\bullet-}$ dismutation. It neutralizes the single charge on the Fe site and in turn reduces favorable electrostatics with the tetracationic (OH)(H_2O)FeP species relative to the pentacationic (H_2O)$_2$MnP species.[6,8,10−13,24] Yet, labilization of the axial water in the trans position relative to OH^- increases largely the reactivity of the Fe site. Consequently, (OH)(H_2O)FePs (with the exception of excessively sterically hindered *n*-octyl *ortho* analogue) have higher k_{cat}($O_2^{\bullet-}$) than (H_2O)$_2$MnPs (Figure 4A,C, Table 4). The interaction between metalloporphyrins and superoxide is outer-sphere with partial inner-sphere character.[12,49] Therefore, the labilization of trans-axial water due to the presence of axial hydroxo ligand has only a modest effect; the difference in the k_{cat}($O_2^{\bullet-}$) between Fe- and Mn porphyrins is in the range of 2.5−5-fold (0.4−0.7 log units). Yet, with reactions of inner-sphere character which involves ligand binding, such as H_2O_2-based degradation, the difference between Fe- and Mn porphyrins is more than an order of magnitude larger (see under Stability toward Oxidative Degradation).

dx.doi.org/10.1021/ic3012519 | *Inorg. Chem.* 2013, 52, 5677−5691

The axially ligated hydroxo ligand affects more the thermodynamic properties of both *ortho* and *meta* (OH)(H_2O)FePs than the polarity/apolarity of alkyl chains; consequently $E_{1/2}$ varies little between *ortho* methyl and *ortho* *n*-octyl (OH)(H_2O)FeP species, while a significant increase in $E_{1/2}$ of ~160 mV was seen from *ortho* methyl to *ortho* *n*-octyl $(H_2O)_2$MnPs (Figure 4B). Further, $E_{1/2}$ varies much less between *ortho* and *meta* (OH)(H_2O)FePs (116−170 mV) than *ortho* and *meta* $(H_2O)_2$MnPs (168−293 mV) (Figure 4B,D, Table 4). Consequently *meta* (OH)(H_2O)FePs with higher $E_{1/2}$ and k_{cat} are more potent SOD mimics than *meta* $(H_2O)_2$MnPs (Table 4, Figure 4C). In *meta* series of both porphyrins though, the $E_{1/2}$ does not change as dramatically with lengthening of alkyl chains as it does with *ortho* analogues; the same is true for log k_{cat} (Figure 5). The reversed trend is seen between $E_{1/2}$ vs nC and log $k_{cat}(O_2^{\bullet-})$ vs nC relationships (Figure 4C,D). The small increase in $E_{1/2}$ of (OH)(H_2O)FePs from methyl to *n*-octyl could not have compensated for steric hindrance; consequently, the log k_{cat} of *ortho* (OH)(H_2O)FePs with shorter methyl and ethyl chains first increases as the trans axial position is activated and more reactive to $O_2^{\bullet-}$, but it decreases then due to the steric hindrance of the longer alkyl chains (Figure 4A). Minor effects are seen with *meta* isomers (Figure 4C) as are further reflected in structure−activity relationships (Figure 5).

Differences in the effect of alkyl substituents upon thermodynamics and kinetics of $O_2^{\bullet-}$ dismutation result in entirely different structure activity relationships (SAR) between the log $k_{cat}(O_2^{\bullet-})$ and $E_{1/2}$ for isomeric Fe and Mn porphyrins (Figure 5). The large increases in $E_{1/2}$ with the alkyl chain length in *ortho* Mn porphyrins (Figure 4B) compensate for the sterically unfavorable effects of longer alkyl-chain analogues on superoxide approach; after initial k_{cat} drop from methyl to *n*-butyl analogue, k_{cat} increases from *n*-butyl to *n*-octyl (Figure 5, left). With Fe porphyrins, there is essentially no major increase in $E_{1/2}$ as the alkyl chains lengthen (Figure 4B); consequently steric effects predominate and determine the shape of SAR (Figure 5, left). While the total change in log k_{cat} is ~1 log unit with *ortho* porphyrins, with *meta* analogues, the total change in k_{cat} is only ~0.2 log units within each of the methyl to *n*-octyl series of Fe and Mn porphyrins (Figures 4A,C and 5); yet the behavior of *meta* MnPs is reversed from the one seen with *ortho* analogues as a consequence of interplay of thermodynamic and kinetics factors. With *meta* Mn porphyrins, the $E_{1/2}$ decreases from *n*-butyl to *n*-octyl much more than with *meta* Fe porphyrins (Figure 4C), and this in turn dominates the SAR.

Stability toward Oxidative Degradation. Given high millimolar intracellular levels of ascorbate and the significance of H_2O_2 as a major *in vivo* signaling (nM) and cytotoxic species (mM), we routinely address the interactions of metalloporphyrins with these species.[21,34,50,51] Cationic Mn and Fe *N*-substituted pyridylporphyrins readily couple with ascorbate catalyzing its oxidation (Figure 6). The catalysis results in H_2O_2 production and subsequent porphyrin degradation. The therapeutic potential of such a system for anticancer therapy via production of long-lasting, highly cytotoxic peroxide was demonstrated.[34,50] Metalloporphyrins have widely been explored in cyt P450 biomimetic models.[52−67] The metalloporphyrin/ascorbate system was proposed by us as a potential *in situ* cyt P450 mimicking system for hydroxylation of cyclophosphamide to its active metabolite 4-hydroxycyclophosphamide.[33]

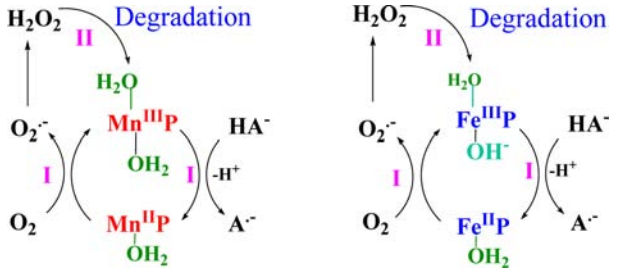

Figure 6. Metalloporphyrin-catalyzed ascorbate (HA^-) oxidation at pH 7.8, leading to the production of $O_2^{\bullet-}$ and H_2O_2 (process I) and subsequent metalloporphyrin oxidative degradation (process II). Peroxide can also be produced in oxidation of metalloporphyrin and ascorbyl radical ($A^{\bullet-}$) with $O_2^{\bullet-}$ (see ref 33; also eqs 5 and 7), $A^{\bullet-}$ with O_2 (producing $O_2^{\bullet-}$) and self-dismutation of $O_2^{\bullet-}$.

Herein we have addressed the H_2O_2-based degradation of *ortho* and *meta* Mn and Fe porphyrins, bearing short ethyl and long *n*-hexyl chains. Metal center/ascorbate was a producer of peroxide. The lower $E_{1/2}$ of *meta* metalloporphyrins relative to *ortho* analogues indicates their preference of higher +3 relative to lower +2 Mn oxidation state. Thus, once reduced with ascorbate, *meta* Mn porphyrins readily reoxidize with oxygen producing more H_2O_2 and are in turn more degradable than *ortho* species. The $k(H_2O_2)$ is 1.3 M^{-1} s^{-1} for $(H_2O)_2$MnTM(E)-2-PyP^{5+} and 4.9 M^{-1} s^{-1} for $(H_2O)_2$MnTM(E)-3-PyP^{5+}.[8] The extensive degradation of porphyrins coincides with spectrophotometric evidence of complete consumption of ascorbate. Ascorbyl radical, $A^{\bullet-}$, formed during reduction of Mn porphyrin, readily oxidizes further to dehydroascorbate producing $O_2^{\bullet-}$, which upon dismutation gives rise to H_2O_2. The Fe porphyrins are much more potent catalysts of ascorbate oxidation than analogous Mn porphyrins due to the labilization of trans-axial water which greatly increases their reactivity in reactions of inner-sphere character (Figure 7). During catalysis, peroxide is formed and its binding and subsequent porphyrin oxidation leads to porphyrin degradation and Fe release. The $k(H_2O_2)$ is 23 M^{-1} s^{-1} for (OH)(H_2O)FeTM(E)-2-PyP^{4+} and is ~20-fold higher relative to $(H_2O)_2$MnTM(E)-2-PyP^{5+}.[8]

Lipophilicity. We have previously reported that *meta* Mn porphyrins are more lipophilic than their *ortho* isomers and showed here that the same is valid for Fe porphyrins (Figure 8). When Fe and Mn porphyrins bear shorter methyl and ethyl chains, the overall charge of the complex is largely exposed to the solvent, making them highly hydrophilic. As the chains lengthen, the impact of the metal site charge is surpassed by the effect of the alkyl chains, and both Fe and Mn porphyrins become similarly lipophilic (Table 5, Figure 8). It is worth noting that the difference in lipophilicity between Fe and Mn porphyrins among the shorter alkyl side-chains is more pronounced in the *meta* than in the *ortho* isomers; this is likely related to the higher exposure of the metal center in the *meta* isomers when compared to their *ortho* analogues, which allows a better differentiation and greater impact of the "$[(H_2O)_2Fe]^{+}$" and "$[(H_2O)_2Mn]^{+}$" moieties on the overall lipophilicity of the complexes. Under physiological conditions, Fe porphyrins exist predominantly as tetracationic (OH)(H_2O)-FeP^{4+} species which makes them more lipophilic than the corresponding Mn porphyrins which, having water as axial ligands, bear an overall 5+ charge, $(H_2O)_2MnP^{5+}$. The impact of the 1 unit reduction from 5+ to 4+ in overall charge of the complexes on their lipophilicity and biological efficiency has been demonstrated in the $Mn^{III}P^{5+}$ and $Mn^{II}P^{4+}$ systems.[69]

dx.doi.org/10.1021/ic3012519 | *Inorg. Chem.* 2013, 52, 5677−5691

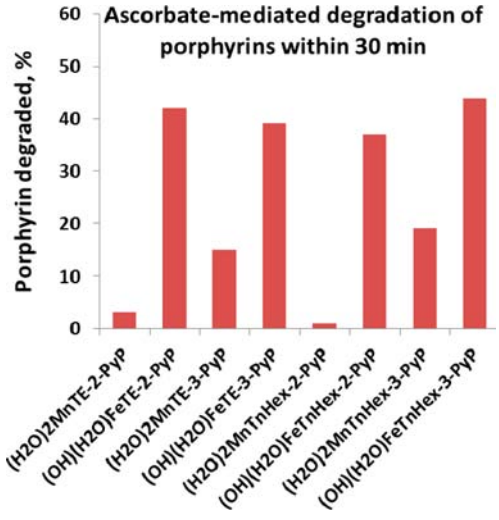

Figure 7. The stability of Fe vs Mn porphyrins toward ascorbate-mediated oxidative degradation at pH 7.8 as shown in Figure 6.[20,33,34,68] The conditions were 6 μM metalloporphyrin, 0.42 mM sodium ascorbate at pH 7.8 maintained with 0.05 M Tris buffer.

Effect of Fe Porphyrins on the Aerobic Growth of SOD-Deficient *E. coli*. The aerobic growth of *E. coli* in the presence of *ortho* (OH)(H_2O)FeTE-2-PyP^{4+} and *meta* (OH)-(H_2O)FeTE-3-PyP^{4+} and our standard SOD mimics *ortho* $(H_2O)_2$MnTE-2-PyP^{5+} is shown in Figure 9. The more lipophilic long-alkyl chain (*n*-hexyl and *n*-octyl) Mn and Fe porphyrins are much more toxic to *E. coli* than the hydrophilic analogues. The fairly lipophilic *n*-butyl porphyrin, (OH)(H_2O)-FeTnBu-2-PyP^{4+}, already starts exerting toxicity at 1 μM.

Ortho $(H_2O)_2$MnTE-2-PyP^{5+} is commonly used as a positive control at 20 μM. At such concentration, it allowed SOD-deficient *E. coli* to grow aerobically in restricted, 5 AA medium at a rate comparable to that of the parental strain.[41] Whereas at concentrations >1 μM (OH)(H_2O)FePs start to exert toxicity, at very low concentrations they supported the growth of the SOD-deficient *E. coli*, and at 0.1 and 1 μM it reached the growth rate of the wild type strain. It is worth noting, however, that the growth pattern of the SOD-deficient strain in medium supplemented with (OH)(H_2O)FeP was different from the growth of wild type *E. coli* or the growth of the *sodAsodB* strain in $(H_2O)_2$MnP-supplemented medium (Figure 9B). Growth

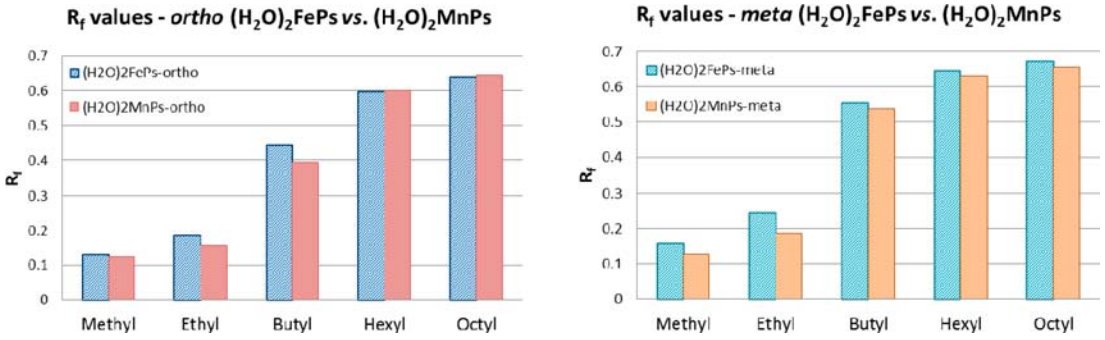

Figure 8. Lipophilicity of Fe and Mn porphyrins as described by chromatographic retention factor, R_f. Data relate to pH 2 and thus to identical diaqua species of both metalloporphyrins (see Table 5). Shorter-chain $(H_2O)_2$FePs are slightly more lipophilic than isomeric $(H_2O)_2$MnPs; as the chains lengthen, their influence on the lipophilicity prevails over charge/ligation at the metal site.

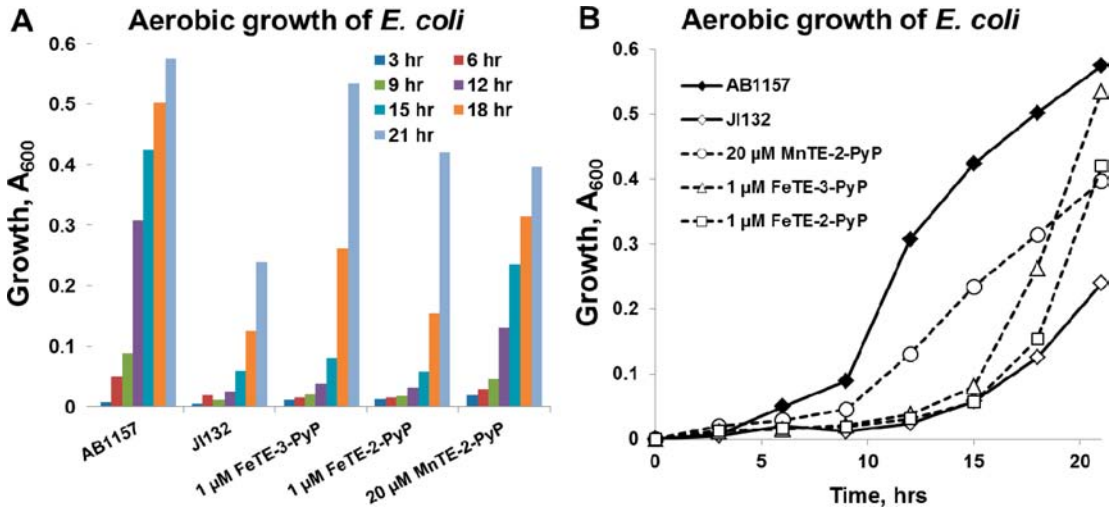

Figure 9. Growth of SOD-deficient JI132 and wild type AB1157 *E. coli* in restricted, five amino-acid medium in the presence or absence of isomeric Fe and Mn porphyrins. In the concentration range of 0.01−1 μM (1 μM is shown only), (OH)(H_2O)FePs stimulated the growth of the SOD-deficient *E. coli*. MnP stimulates *E. coli* growth at concentrations >5 μM (A). Growth curves, demonstrating differences in growth pattern (B); in the presence of $(H_2O)_2$MnPs JI132 starts to growth simultaneously with the SOD-proficient strain. In contrast, (OH)(H_2O)FePs does not shorten the lag period but helps the growth of JI132 after it had already overcome the growth lag.

dx.doi.org/10.1021/ic3012519 | *Inorg. Chem.* 2013, 52, 5677−5691

curves show that in the presence of $(H_2O)_2$MnPs, the SOD-deficient mutant started growth simultaneously with the SOD-proficient parent. In a medium supplemented with (OH)-(H_2O)FeP, however, growth was delayed and did not start earlier than in a nonsupplemented 5AA medium. Only after a prolonged lag period was $(OH)(H_2O)$FeP capable of stimulating the growth of the mutant to a rate comparable to that of the SOD-proficient parent. Such data suggest that $(OH)(H_2O)$FeP stimulates the growth of the SOD-deficient *E. coli* by a mechanism different than that of $(H_2O)_2$MnP despite the fact that the two compounds have similar $k_{cat}(O_2^{\bullet-})$, $E_{1/2}$ and lipophilicity (Tables 4 and 5).

In a cell-free test tube Fe porphyrins are rapidly degraded by hydrogen peroxide with release of Fe^{2+}. A similar process can occur *in vivo*. Organisms contain millimolar concentrations of cellular reductants (ascorbate, glutathione and other thiols, etc.) which are readily oxidized by Fe and Mn porphyrins acting as catalysts.[21,34] A product of such reactions is hydrogen peroxide, which rapidly degrades FePs but not MnPs.

To further explore the reasons behind growth stimulation by low concentration of Fe porphyrins, we compared it with the effect of Fe(II) and Mn(II) salts under the same conditions. The Mn porphyrin at 20 μM served as a positive control. Figure 10 shows that at 1 μM Fe(II) citrate stimulated the growth of the SOD-deficient *E. coli* similar to 1 μM Fe porphyrin. Under the conditions of this experiment, Mn-citrate did not improve the growth of any of the SOD-deficient strains (Figure 10). Importantly, the pattern in *E. coli* growth with Mn porphyrins and Fe salts is essentially the same (Figure 10).

To check if indeed the Fe porphyrin is degraded during *E. coli* growth, cytosolic fractions of *sodAsodB E. coli* grown in a medium supplemented with either Fe or Mn porphyrin were analyzed over a 12 h period. Judging by the disappearance of the Soret band, no loss of Mn porphyrin occurred during the examination period, while the Fe porphyrin almost completely disappeared from the *E. coli* cytosol (Figure 11) and from the medium (data not shown). The time interval needed for SOD-deficient *E. coli* to start growing coincides with the Fe porphyrin almost complete degradation period (Figure 10 and 11). Therefore, growth stimulation by the Fe porphyrin should be

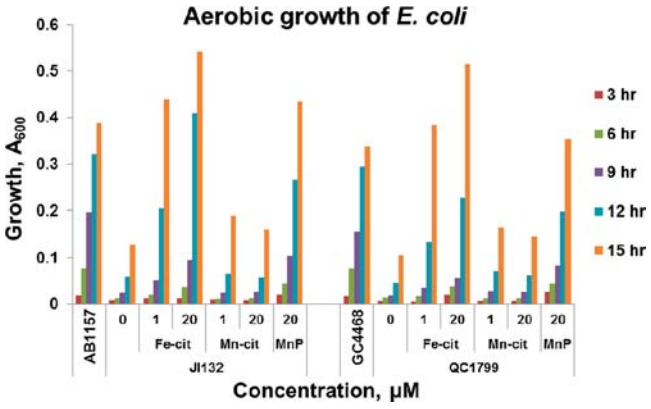

Figure 10. Comparison of the effect of Fe(II) citrate and Mn(II) citrate on growth of two different SOD-deficient strains, JI1132 and QC1799, in 5AA medium. The metal salts were used at concentrations of 1 and 20 μM. The same effect was observed with other Mn and Fe salts (sulfates and chlorides). The growth of SOD-proficient strains (AB1157 and GC4468) and their SOD-deficient analogues (JI132 and QC1799) in the absence of metal salts and metalloporphyrins is shown also.

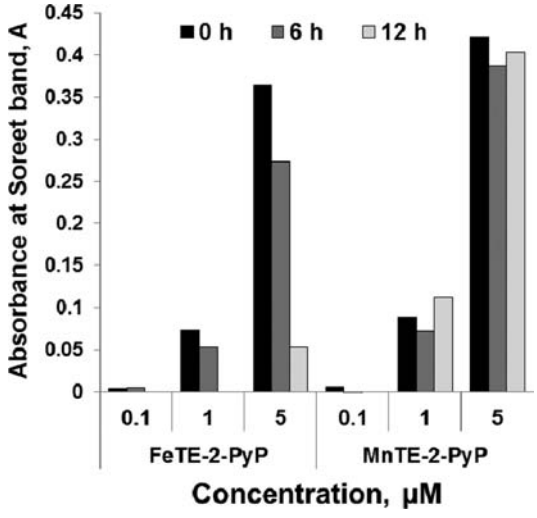

Figure 11. The disappearance of FeTE-2-PyP^{5+} from the cytosol of *E. coli* during the 12-h growth in 5AA medium. Absorbances of Soret band were given and relate to the different initial concentrations of Fe porphyrin. For comparison the data on Mn porphyrin, MnTE-2-PyP^{5+} were given also.

Scheme 1. The Differential Aspects of the *in Vivo* Mechanisms of Action of Fe and Mn Porphyrins[a]

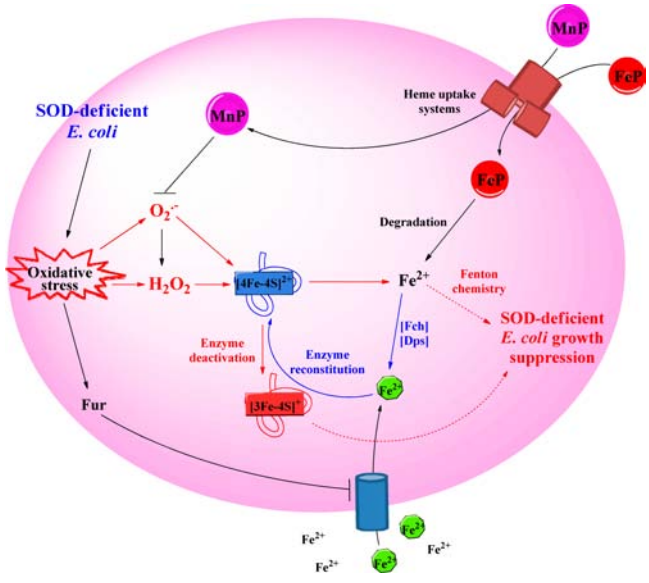

[a]The proposed mechanisms are based on the aerobic growth of SOD-deficient *E. coli*. Mn and Fe porphyrins are presumably uptaken by a heme transport mechanism. Subsequently FePs undergo rapid degradation due to fast redox cycling with cellular reductants whereby "free" Fe^{2+} is released. Fe^{2+} is readily chelated to iron-transporting/sequestering siderophores (e.g., [Fch] - ferrochelatase; [Dps] - Fe-storage protein; indicated as green circles). At very low levels, Fe^{2+} could reconstitute [4Fe-4S] clusters of enzymes, such as aconitases. These enzymes undergo superoxide-driven oxidative degradation and subsequent, yet reversible release of Fe^{2+}. At high concentration of Fe^{2+}, the deleterious effects of Fenton chemistry ·OH radical production prevail. The MnPs, however, due to their different chemistry when compared to FePs are more resistant towards oxidative degradation and protect *E. coli* by scavenging superoxide whereby preventing its damaging effect upon different [4Fe-4S] clusters-containing enzymes.

dx.doi.org/10.1021/ic3012519 | *Inorg. Chem.* 2013, 52, 5677−5691

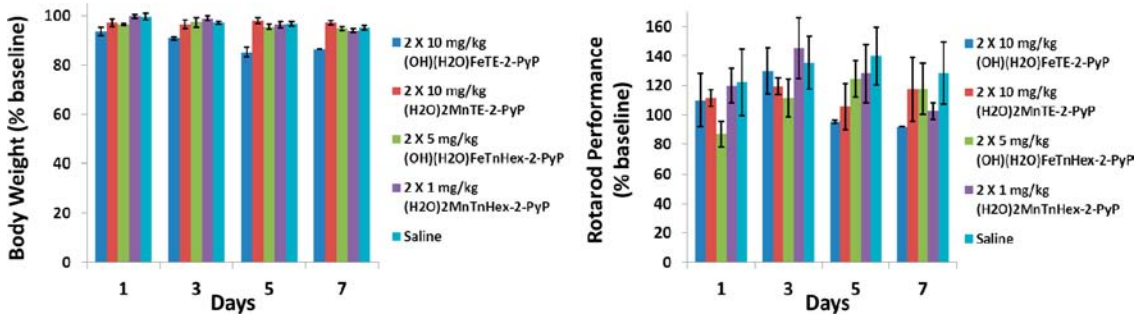

Figure 12. Comparison of the effects of Fe- and Mn porphyrins on mouse performance and weight. The behavior, weights and rotarod performances were followed daily. The compounds were tested at doses which cause no or marginal, transient toxicity: $(OH)(H_2O)$FeTE-2-PyP^{4+} (2 × 10 mg/kg/day), $(H_2O)_2$MnTE-2-PyP^{5+} (2 × 10 mg/kg/day), $(OH)(H_2O)$FeTnHex-2-PyP^{4+} (2 × 5 mg/kg/day) and $(H_2O)_2$MnTnHex-2-PyP^{5+} (2 × 1 mg/kg/day).

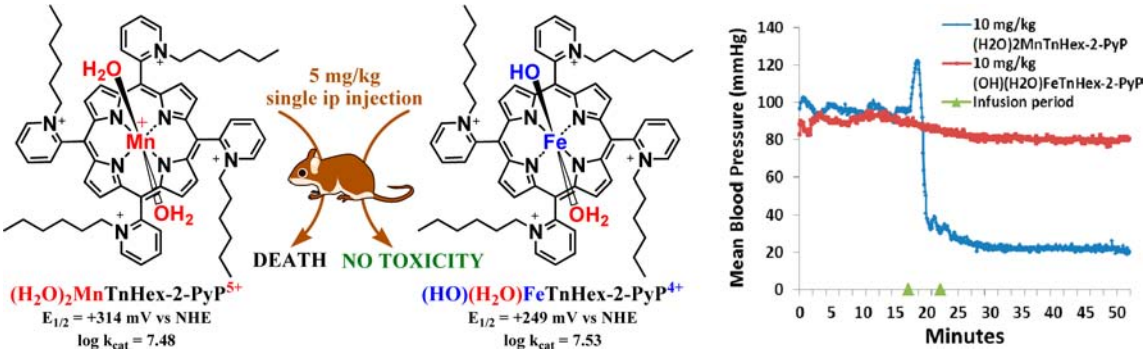

Figure 13. The comparison of the mouse effects of Fe- and Mn porphyrins. At 5 mg/kg single ip injection all 4 tested mice died within 2 h with $(H_2O)_2$MnTnHex-2-PyP^{5+} while two daily ip injections of 5 mg/kg of $(OH)(H_2O)$FeTnHex-2-PyP^{4+} for a week was well tolerated. Changes in systolic blood pressure were monitored for an hour after intravenous injection of 10 mg/kg of either metalloporphyrin. No arterial hypotension was observed with either $(OH)(H_2O)$FeTnHex-2-PyP^{4+} or $(OH)(H_2O)$FeTE-2-PyP^{4+} (data for ethyl (E) analogue not shown).

attributed to facilitation of microbial iron acquisition, rather than to Fe porphyrin acting as an SOD mimic.

Several enzymes, which include dihydroxy acid dehydratase, aconitase, 6-phosphogluconate dehydratase, and fumarases A and B, are oxidatively damaged by superoxide.[70−74] As a result Fe^{2+} is released from the $[4Fe\text{-}4S]^{2+}$ clusters and the enzymes are inactivated. The Fe^{2+} added exogenously may reconstitute these enzymes and restore their activity.[75] Our data demonstrate a remarkable difference in the behavior of Fe vs Mn porphyrin as a direct consequence of large difference in their reactivities (as exemplified with ∼18-fold faster peroxide-based degradation of Fe porphyrin) which in turn is a consequence of 5 log units difference in the electron-deficiency of the metal site. Therefore, the rapid degradation of Fe porphyrins *in vivo* with peroxide *per se* or peroxide produced while redox-cycling with cellular reductants[21,25,32] may have a major effect on their mechanism of action.

Although efficacious at low concentrations (0.01−1 μM) Fe porphyrins become toxic at >1 μM (Figure 11). In contrast, Fe(II) salts promote the SOD-deficient *E. coli* growth even at 20 μM. This phenomenon is likely related to different transport mechanisms that *E. coli* employs to control the uptake of Fe from the medium. The uptake of "free" Fe is tightly regulated *via* specific compounds — siderophores — which microorganism excretes into the medium.[76−83] Consequently, high amounts of "free" Fe^{2+} (Fe salts) may not be taken up even if present in the medium. Fe porphyrin bypasses such cellular control mechanisms and presumably accumulates within the cell *via* heme-uptake systems.[84,85]

Scheme 1 summarizes the differential aspects of *in vivo* mechanisms of action of Mn and Fe porphyrins as exemplified by the protection of aerobic growth of SOD-deficient *E. coli*.

Mouse Study. We conducted a mouse study for initial comparison of Fe- and Mn porphyrins in mammalian systems. Four porphyrins were tested for toxicity to mice: $(OH)(H_2O)$-FeTE-2-PyP^{4+} (2 × 10 mg/kg/day), $(H_2O)_2$MnTE-2-PyP^{5+} (2 × 10 mg/kg/day), $(OH)(H_2O)$FeTnHex-2-PyP^{4+} (2 × 5 mg/kg/day) and $(H_2O)_2$MnTnHex-2-PyP^{5+} (2 × 1 mg/kg/day). In most *in vivo* studies, several fold lower doses of Fe porphyrins than Mn porphyrins were used.[3,4,86−88] To obtain stronger response, we tested both Fe- and Mn porphyrins at comparable doses (in *E. coli* the nontoxic doses of Fe porphyrins are 10−1000-fold lower than those of Mn porphyrins). While not anticipated, significant toxic effects were observed with $(OH)(H_2O)$FeTE-2-PyP^{4+}. The nature of those effects is not yet understood.

Unexpectedly, $(OH)(H_2O)$FeTnHex-2-PyP^{4+} appears less toxic than its Mn counterpart, $(H_2O)_2$MnTnHex-2-PyP^{5+} (Figures 12 and 13). While with 5 mg/kg single injection of $(H_2O)_2$MnTnHex-2-PyP^{5+} all four mice died,[23] with (OH)-(H_2O)FeTnHex-2-PyP^{4+} no significant toxicity was seen in 4 out of 5 mice (one mouse died). These compounds have similar lipophilicity. It is tempting to speculate that axial hydroxo vs axial aqua ligand affects differentially the interaction of Fe- and Mn porphyrins with biological targets which in turn leads to differences in toxicity. It should be noted, however, that long-alkyl chains hinder the impact of the type of axial ligand analogues in all atropoisomers, except *αααα*. Another major difference between the Mn and Fe porphyrins is the absence of

dx.doi.org/10.1021/ic3012519 | *Inorg. Chem.* 2013, 52, 5677−5691

a net positive charge on Fe site, as it is neutralized by the presence of the axial hydroxo ligand.

Fe- and Mn porphyrins had different effects on mice blood pressure (Figure 13). It is known that Mn porphyrins cause hypotension,[89] and dramatic drop of blood pressure was observed when $(H_2O)_2$MnTnHex-2-PyP^{5+} was injected (Figure 13). In contrast, none of the tested Fe porphyrins exerted hypotensive effect on mice. The hypotensive action of the Mn porphyrins was strongly influenced by the length of the alkyl chain at pyridyl ring. Thus, $(H_2O)_2$MnTnHex-2-PyP^{5+} was the strongest and $(H_2O)_2$MnTE-2-PyP^{5+} was the weakest hypotensive agent. The difference in axial coordination may not play major role either. Metal site is less hindered and more exposed in short chain ethyl analogs, $(H_2O)_2$MnTE-2-PyP^{5+} and (OH)(H_2O)FeTE-2-PyP^{4+}, thus the differential effect of axial hydroxo vs aqua ligand in their interactions with biological target should have been mostly pronounced. However, a weak hypotensive effect was observed with $(H_2O)_2$MnTE-2-PyP^{5+} and no hypotension with (OH)(H_2O)FeTE-2-PyP^{4+}. With *n*-hexyl compounds, the long chains form a cavity around the metal center, and axial ligation may not play a role other than in *αααα* atropoisomer. With both Fe and Mn *n*-hexyl analogues, the interaction with biological targets should be dominated by similar hydrophobic nature of long alkyl chains. The nature of systemic toxicity of Fe vs Mn porphyrin is, thus, not yet understood and requires clearly further exploration.

CONCLUSIONS

Water-soluble Mn(III) *N*-alkylpyridylporphyrins, $(H_2O)_2$MnPs are bis-aqua complexes under physiological conditions, while the analogous Fe porphyrins (OH)(H_2O)FePs have a hydroxo axial ligand trans axially coordinated to water molecule. As a consequence the Fe site has 5 log units lower electron density than its Mn analogue, which determines the differences between Fe and Mn porphyrins in redox chemistry, reactivity, and biological actions. The presence of hydroxo ligand labilizes trans-axial water which increases the reactivity of Fe porphyrin in comparison with the Mn porphyrin center. This was demonstrated *in vitro* and *in vivo* with *E. coli*. In the presence of high millimolar levels of cellular reductants (ascorbate, glutathione, cysteine, etc.) and/or peroxide, Fe porphyrins are rapidly degraded releasing "free" Fe^{2+}. In contrast to Mn porphyrin, delivery of iron but not the Fe porphyrin itself stimulated the growth of the SOD-deficient *E. coli*. The relevance of such intriguing biochemistry of Fe porphyrins to eukaryotic systems is under further exploration to understand the favorable effects of Fe porphyrins often reported in animal models of oxidative stress injuries.[2,3,88,90]

AUTHOR INFORMATION

Corresponding Authors

*(I.B.-H.) Address: Department of Radiation Oncology, Duke University Medical Center, Durham, NC 27710. Tel: 919-684-2101. E-mail: ibatinic@duke.edu. (L.B.) Address: Kuwait University, Faculty of Medicine, Department of Biochemistry, Jabriya, 4th floor, Rm 48 13110 Safat, Kuwait. E-mail: lbenov@HSC.EDU.KW.

Notes

The authors declare no competing financial interest.

ACKNOWLEDGMENTS

Authors acknowledge financial help from W.H. Coulter Translational Partners Grant Program (I.B.H., I.S., A.T.), and NIH/NCI Duke Comprehensive Cancer Center Core Grant (5-P30-CA14236-29) (I.S.), NIH U19AI067798, The Robert Preston Tisch Brain Tumor Center at Duke Developmental Career Award to IBH, and IBH general research funds (A.T., Z.R., T.W.). J.S.R. thanks CNPq and UFPB. I.B.H., D.S.W., and I.S. are consultants with BioMimetix Pharmaceutical, Inc. L.B. acknowledges the financial support from Kuwait University, Grant MB01/09, the excellent technical assistance of Milini Thomas, and Research Core Facility Grants GM01/01 and GM01/05.

ABBREVIATIONS

$ONOO^-$, peroxynitrite; $O_2^{\bullet-}$, superoxide only porphyrin ligands are listed here; H_2TM-2(or 3)-PyP^{4+}, *meso*-tetrakis(*N*-methylpyridinum-2(or 3)-yl)porphyrin; H_2TE-2(or 3)-PyP^{4+}, *meso*-tetrakis(*N*-ethylpyridinum-2(or 3)-yl)porphyrin; H_2TnBu-2(or 3)-PyP^{4+}, *meso*-tetrakis(*N*-*n*-butylpyridinum-2(or 3)-yl)porphyrin; H_2TnHex-2(or 3)-PyP^{4+}, *meso*-tetrakis-(*N*-*n*-hexylpyridinum-2(or 3)-yl)porphyrin; H_2TnOct-2(or 3)-PyP^{4+}, *meso*-tetrakis(*N*-*n*-octylpyridinum-2(or 3)-yl)porphyrin; when used, FeP and MnP abbreviations do not imply axial ligation; $(H_2O)_2$MnPs, diaqua Mn(III) *N*-alkylpyridylporphyrins and (OH)(H_2O)FePs and $(H_2O)_2$FePs, monohydroxo-monoaqua and diaqua Fe(III) *N*-alkylpyridylporphyrins, respectively, no charges are indicated for simplicity; MnTE-2-PyP^{5+}, AEOL10113, Mn(III) *meso*-tetrakis(*N*-ethylpyridinum-2-yl)-porphyrin; FeTM-4-PyP^{4+}, Fe(III) *meso*-tetrakis(*N*-methylpyridinum-4-yl)porphyrin; FP-15, Fe(III) *meso*-tetrakis(*N*-(1-(2-(2-(2-methoxyethoxy)ethoxy)ethyl)pyridinium-2-yl)porphyrin; INO-4885, the structure of WW-85 has not been made available in *J. Pharmacol. Exp. Ther.*; DMF, *N*,*N*-dimethylformamide; HFBA, heptafluorobutyric acid; R_f, thin-layer chromatographic retention factor that presents the ratio between the solvent and compound path in acetonitrile/$KNO_{3(sat)}$/H_2O = 8:1:1 solvent system; $E_{1/2}$, half-wave reduction potential; SOD, superoxide dismutase; NHE, normal hydrogen electrode; P_{OW}, partition coefficient between *n*-octanol and water; HA^-, monodeprotonated ascorbic acid; $A^{\bullet-}$, ascorbyl radical; MTD, maximal tolerable dose; charges omitted in some figures.

REFERENCES

(1) Genovese, T.; Mazzon, E.; Esposito, E.; Di Paola, R.; Murthy, K.; Neville, L.; Bramanti, P.; Cuzzocrea, S. *Free Radic. Res.* **2009**, *43* (7), 631−645.

(2) Lange, M.; Szabo, C.; Enkhbaatar, P.; Connelly, R.; Horvath, E.; Hamahata, A.; Cox, R. A.; Esechie, A.; Nakano, Y.; Traber, L. D.; Herndon, D. N.; Traber, D. L. *Am. J. Physiol. Lung Cell Mol. Physiol.* **2011**, *300* (2), L167−L175.

(3) Maybauer, D. M.; Maybauer, M. O.; Szabo, C.; Cox, R. A.; Westphal, M.; Kiss, L.; Horvath, E. M.; Traber, L. D.; Hawkins, H. K.; Salzman, A. L.; Southan, G. J.; Herndon, D. N.; Traber, D. L. *Shock* **2011**, *35* (2), 148−155.

(4) Maybauer, D. M.; Maybauer, M. O.; Szabo, C.; Westphal, M.; Traber, L. D.; Salzman, A. L.; Herndon, D. N.; Traber, D. L. *Burns* **2011**, *37* (5), 842−850.

(5) Pieper, G. M.; Nilakantan, V.; Chen, M.; Zhou, J.; Khanna, A. K.; Henderson, J. D., Jr.; Johnson, C. P.; Roza, A. M.; Szabo, C. *J. Pharmacol. Exp. Ther.* **2005**, *314* (1), 53−60.

(6) Batinic-Haberle, I.; Reboucas, J. S.; Benov, L.; Spasojevic, I., Chemistry, biology and medical effects of water soluble metalloporphyrins. In *Handbook of Porphyrin Science*; Kadish, K. M., Smith, K. M., Guillard, R., Eds.; World Scientific: Singapore, 2011; Vol. *11*, pp 291−393.

(7) Szabo, C.; Mabley, J. G.; Moeller, S. M.; Shimanovich, R.; Pacher, P.; Virag, L.; Soriano, F. G.; Van Duzer, J. H.; Williams, W.; Salzman, A. L.; Groves, J. T. *Mol. Med.* **2002**, *8* (10), 571−580.
(8) Batinić-Haberle, I.; Spasojević, I.; Hambright, P.; Benov, L.; Crumbliss, A. L.; Fridovich, I. *Inorg. Chem.* **1999**, *38* (18), 4011−4022.
(9) Batinic-Haberle, I.; Benov, L.; Spasojevic, I.; Fridovich, I. *J. Biol. Chem.* **1998**, *273* (38), 24521−24528.
(10) Batinic-Haberle, I.; Rajic, Z.; Tovmasyan, A.; Reboucas, J. S.; Ye, X.; Leong, K. W.; Dewhirst, M. W.; Vujaskovic, Z.; Benov, L.; Spasojevic, I. *Free Radic. Biol. Med.* **2011**, *51* (5), 1035−1053.
(11) Batinic-Haberle, I.; Reboucas, J. S.; Spasojevic, I. *Antioxid. Redox Signal* **2010**, *13* (6), 877−918.
(12) Reboucas, J. S.; DeFreitas-Silva, G.; Spasojevic, I.; Idemori, Y. M.; Benov, L.; Batinic-Haberle, I. *Free Radic. Biol. Med.* **2008**, *45* (2), 201−210.
(13) Spasojevic, I.; Batinic-Haberle, I.; Reboucas, J. S.; Idemori, Y. M.; Fridovich, I. *J. Biol. Chem.* **2003**, *278* (9), 6831−6837.
(14) Batinic-Haberle, I.; Spasojevic, I.; Tse, H. M.; Tovmasyan, A.; Rajic, Z.; St Clair, D. K.; Vujaskovic, Z.; Dewhirst, M. W.; Piganelli, J. D. *Amino Acids* **2010**, *42*, 95−113.
(15) Miriyala, S.; Spasojevic, I.; Tovmasyan, A.; Salvemini, D.; Vujaskovic, Z.; St Clair, D.; Batinic-Haberle, I. *Biochim. Biophys. Acta* **2012**, *1822* (5), 794−814.
(16) Tovmasyan, A.; Sheng, H.; Weitner, T.; Arulpragasam, A.; Lu, M.; Warner, D. S.; Spasojevic, I.; Batinic-Haberle, I. *Med. Princ. Pract.* **2013**, *22*, 103−130.
(17) Kos, I.; Reboucas, J. S.; DeFreitas-Silva, G.; Salvemini, D.; Vujaskovic, Z.; Dewhirst, M. W.; Spasojevic, I.; Batinic-Haberle, I. *Free Radic. Biol. Med.* **2009**, *47* (1), 72−78.
(18) Pinto, V. H.; Carvalhoda-Silva, D.; Santos, J. L.; Weitner, T.; Fonseca, M. G.; Yoshida, M. I.; Idemori, Y. M.; Batinic-Haberle, I.; Reboucas, J. S. *J. Pharm. Biomed. Anal.* **2013**, *73*, 29−34.
(19) Reboucas, J. S.; Spasojevic, I.; Batinic-Haberle, I. *J. Pharm. Biomed. Anal.* **2008**, *48* (3), 1046−1049.
(20) Tovmasyan, A. G.; Rajic, Z.; Spasojevic, I.; Reboucas, J. S.; Chen, X.; Salvemini, D.; Sheng, H.; Warner, D. S.; Benov, L.; Batinic-Haberle, I. *Dalton Trans.* **2011**, *40* (16), 4111−4121.
(21) Ferrer-Sueta, G.; Batinic-Haberle, I.; Spasojevic, I.; Fridovich, I.; Radi, R. *Chem. Res. Toxicol.* **1999**, *12* (5), 442−449.
(22) Spasojevic, I.; Batinic-Haberle, I.; Stevens, R. D.; Hambright, P.; Thorpe, A. N.; Grodkowski, J.; Neta, P.; Fridovich, I. *Inorg. Chem.* **2001**, *40* (4), 726−739.
(23) Rajic, Z.; Tovmasyan, A.; Spasojevic, I.; Sheng, H.; Lu, M.; Li, A. M.; Gralla, E. B.; Warner, D. S.; Benov, L.; Batinic-Haberle, I. *Free Radic. Biol. Med.* **2012**, *52* (9), 1828−1834.
(24) Rodgers, K. R.; Reed, R. A.; Su, Y. O.; Spiro, T. G. *Inorg. Chem.* **1992**, *31* (13), 2688−2700.
(25) Ferrer-Sueta, G.; Vitturi, D.; Batinic-Haberle, I.; Fridovich, I.; Goldstein, S.; Czapski, G.; Radi, R. *J. Biol. Chem.* **2003**, *278* (30), 27432−27438.
(26) Weitner, T.; Budimir, A.; Kos, I.; Batinic-Haberle, I.; Birus, M. *Dalton Trans.* **2010**, *39* (48), 11568−11576.
(27) Chen, S.-M.; Sun, P.-J.; Su, Y. O. *J. Electroanal. Chem. Interfacial Electrochem.* **1990**, *294* (1−2), 151−164.
(28) Forshey, P. A.; Kuwana, T. *Inorg. Chem.* **1981**, *20* (3), 693−700.
(29) Kobayashi, N. *Inorg. Chem.* **1985**, *24* (21), 3324−3330.
(30) Kobayashi, N.; Koshiyama, M.; Osa, T.; Kuwana, T. *Inorg. Chem.* **1983**, *22* (24), 3608−3614.
(31) Tondreau, G. A.; Wilkins, R. G. *Inorg. Chem.* **1986**, *25* (16), 2745−2750.
(32) Tovmasyan, A.; Weitner, T.; Roberts, E.; Jaramillo, M.; Spasojevic, I.; Leong, K.; Tome, M.; Benov, L.; Batinic-Haberle, I. *Free Radic. Biol. Med.* **2012**, *53* (2), S120.
(33) Spasojevic, I.; Colvin, O. M.; Warshany, K. R.; Batinic-Haberle, I. *J. Inorg. Biochem.* **2006**, *100* (11), 1897−1902.
(34) Ye, X.; Fels, D.; Tovmasyan, A.; Aird, K. M.; Dedeugd, C.; Allensworth, J. L.; Kos, I.; Park, W.; Spasojevic, I.; Devi, G. R.; Dewhirst, M. W.; Leong, K. W.; Batinic-Haberle, I. *Free Radic. Res.* **2011**, *45* (11−12), 1289−1306.
(35) Al-Maghrebi, M.; Fridovich, I.; Benov, L. *Arch. Biochem. Biophys.* **2002**, *402* (1), 104−109.
(36) Brown, O. R.; Smyk-Randall, E.; Draczynska-Lusiak, B.; Fee, J. A. *Arch. Biochem. Biophys.* **1995**, *319* (1), 10−22.
(37) Benov, L.; Fridovich, I. *J. Biol. Chem.* **1999**, *274* (7), 4202−4206.
(38) Benov, L.; Kredich, N. M.; Fridovich, I. *J. Biol. Chem.* **1996**, *271* (35), 21037−21040.
(39) Imlay, J. A.; Linn, S. *J. Bacteriol.* **1987**, *169* (7), 2967−2976.
(40) Touati, D.; Jacques, M.; Tardat, B.; Bouchard, L.; Despied, S. *J. Bacteriol.* **1995**, *177* (9), 2305−2314.
(41) Kos, I.; Benov, L.; Spasojevic, I.; Reboucas, J. S.; Batinic-Haberle, I. *J. Med. Chem.* **2009**, *52* (23), 7868−7872.
(42) Flynn, C. M. *Chem. Rev.* **1984**, *84* (1), 31−41.
(43) Macartney, D. H.; Sutin, N. *Inorg. Chem.* **1985**, *24* (21), 3403−3409.
(44) Scheidt, W. R.; Cohen, I. A.; Kastner, M. E. *Biochemistry* **1979**, *18* (16), 3546−3552.
(45) Korber, F. C. F.; Smith, J. R. L.; Prince, S.; Rizkallah, P.; Reynolds, C. D.; Shawcross, D. R. *J. Chem. Soc., Dalton Trans.* **1991**, *12*, 3291−3294.
(46) Prince, S.; Korber, F.; Cooke, P. R.; Lindsay Smith, J. R.; Mazid, M. A. *Acta Crystallogr., Sect. C: Cryst. Struct. Commun.* **1993**, *49* (6), 1158−1160.
(47) Aguirre, J. D.; Culotta, V. C. *J. Biol. Chem.* **2012**, *287* (17), 13541−8.
(48) Ramirez-Gutierrez, O.; Claret, J.; Ribo, J. M. *J. Porphyrins Phthalocyanines* **2005**, *9* (6), 436−43.
(49) Batinic-Haberle, I.; Spasojevic, I.; Stevens, R. D.; Hambright, P.; Neta, P.; Okado-Matsumoto, A.; Fridovich, I. *Dalton Trans.* **2004**, *11*, 1696−1702.
(50) Tian, J.; Peehl, D. M.; Knox, S. J. *Cancer Biother. Radiopharm.* **2010**, *25* (4), 439−448.
(51) Tovmasyan, A.; Weitner, T.; Spasojevic, I.; Rajic, Z.; Benov, L.; Batinic-Haberle, I. *Free Radic. Biol. Med.* **2011**, *51*, S99.
(52) Meunier, B.; de Visser, S. P.; Shaik, S. *Chem. Rev.* **2004**, *104* (9), 3947−3980.
(53) Almarsson, O.; Bruice, T. C. *J. Am. Chem. Soc.* **1995**, *117* (16), 4533−4544.
(54) Murata, K.; Panicucci, R.; Gopinath, E.; Bruice, T. C. *J. Am. Chem. Soc.* **1990**, *112* (16), 6072−6083.
(55) Meunier, B.; Bernadou, J. *Top. Catal.* **2002**, *21* (1), 47−54.
(56) Newcomb, M.; Toy, P. H. *Acc. Chem. Res.* **2000**, *33* (7), 449−455.
(57) Aguey-Zinsou, K.-F.; Bernhardt, P. V.; De Voss, J. J.; Slessor, K. E. *Chem. Commun.* **2003**, *3*, 418−419.
(58) Nam, W.-H.; Rhee, S.-W. *ChemInform* **2004**, *35* (50), 201−205.
(59) Nam, W.; Jin, S. W.; Lim, M. H.; Ryu, J. Y.; Kim, C. *Inorg. Chem* **2002**, *41* (14), 3647−3652.
(60) Groves, J. T. *J. Inorg. Biochem.* **2006**, *100* (4), 434−447.
(61) Nam, W.; J. Choi, H.; J. Han, H.; H. Cho, S.; J. Lee, H.; Han, S.-Y. *Chem. Commun.* **1999**, *4*, 387−388.
(62) Song, W.; Ryu, Y.; Song, R.; Nam, W. *J. Biol. Inorg. Chem.* **2005**, *10* (3), 294−304.
(63) Beck, M. J.; Gopinath, E.; Bruice, T. C. *J. Am. Chem. Soc.* **1993**, *115* (1), 21−29.
(64) Arasasingham, R. D.; Bruice, T. C. *J. Am. Chem. Soc.* **1991**, *113* (16), 6095−6103.
(65) Zipplies, M. F.; Lee, W. A.; Bruice, T. C. *J. Am. Chem. Soc.* **1986**, *108* (15), 4433−4445.
(66) Panicucci, R.; Bruice, T. C. *J. Am. Chem. Soc.* **1990**, *112* (16), 6063−6071.
(67) Jeon, S.; Bruice, T. C. *Inorg. Chem.* **1992**, *31* (23), 4843−4848.
(68) Chen, Q.; Espey, M. G.; Sun, A. Y.; Pooput, C.; Kirk, K. L.; Krishna, M. C.; Khosh, D. B.; Drisko, J.; Levine, M. *Proc. Natl. Acad. Sci. U. S. A.* **2008**, *105* (32), 11105−11109.
(69) Spasojevic, I.; Kos, I.; Benov, L. T.; Rajic, Z.; Fels, D.; Dedeugd, C.; Ye, X.; Vujaskovic, Z.; Reboucas, J. S.; Leong, K. W.; Dewhirst, M. W.; Batinic-Haberle, I. *Free Radic. Res.* **2011**, *45* (2), 188−200.

(70) Flint, D. H.; Tuminello, J. F.; Emptage, M. H. *J. Biol. Chem.* **1993**, *268* (30), 22369−22376.
(71) Gardner, P. R.; Fridovich, I. *J. Biol. Chem.* **1991**, *266* (3), 1478−1483.
(72) Gardner, P. R.; Fridovich, I. *J. Biol. Chem.* **1991**, *266* (29), 19328−33.
(73) Kuo, C. F.; Mashino, T.; Fridovich, I. *J. Biol. Chem.* **1987**, *262* (10), 4724−4727.
(74) Liochev, S. I.; Fridovich, I.; Fumarase, C. *Proc. Natl. Acad. Sci. U. S. A.* **1992**, *89* (13), 5892−5896.
(75) Benov, L.; Fridovich, I. *J. Biol. Chem.* **1998**, *273* (17), 10313−10316.
(76) Bagg, A.; Neilands, J. B. *Biochemistry* **1987**, *26* (17), 5471−5477.
(77) Bagg, A.; Neilands, J. B. *Microbiol. Rev.* **1987**, *51* (4), 509−518.
(78) Braun, V. *Int. J. Med. Microbiol.* **2001**, *291* (2), 67−79.
(79) Braun, V. *Front Biosci.* **2003**, *8*, s1409−s1421.
(80) Braun, V.; Killmann, H. *Trends Biochem. Sci.* **1999**, *24* (3), 104−109.
(81) Hantke, K. *FEMS Microbiol. Lett.* **1982**, *15* (2), 83−86.
(82) Kammler, M.; Schon, C.; Hantke, K. *J. Bacteriol.* **1993**, *175* (19), 6212−6219.
(83) Touati, D.; Jacques, M.; Tardat, B.; Bouchard, L.; Despied, S. *J. Bacteriol.* **1995**, *177* (9), 2305−2314.
(84) Anzaldi, L. L.; Skaar, E. P. *Infect. Immun.* **2010**, *78* (12), 4977−4989.
(85) Tong, Y.; Guo, M. *Arch. Biochem. Biophys.* **2009**, *481* (1), 1−15.
(86) Radovits, T.; Beller, C. J.; Groves, J. T.; Merkely, B.; Karck, M.; Szabo, C.; Szabo, G. *Eur. J. Cardiothorac. Surg.* **2012**, *41* (2), 391−396.
(87) Radovits, T.; Seres, L.; Gero, D.; Lin, L. N.; Beller, C. J.; Chen, S. H.; Zotkina, J.; Berger, I.; Groves, J. T.; Szabo, C.; Szabo, G. *Mech. Ageing Dev.* **2007**, *128* (2), 173−181.
(88) Szabo, G.; Loganathan, S.; Merkely, B.; Groves, J. T.; Karck, M.; Szabo, C.; Radovits, T. *J. Thorac. Cardiovasc. Surg.* **2012**, *143*, 1443−1449.
(89) Ross, A. D.; Sheng, H.; Warner, D. S.; Piantadosi, C. A.; Batinic-Haberle, I.; Day, B. J.; Crapo, J. D. *Free Radic. Biol. Med.* **2002**, *33* (12), 1657−1669.
(90) Soriano, F. G.; Lorigados, C. B.; Pacher, P.; Szabo, C. *Shock* **2011**, *35* (6), 560−566.

dx.doi.org/10.1021/ic3012519 | *Inorg. Chem.* 2013, 52, 5677−5691